ELSEVIER

Contents lists available at ScienceDirect

Quaternary International

journal homepage: www.elsevier.com/locate/quaint





Evidence of destructive debris flows at (pre-) Hispanic Cayambe settlements, Ecuador

Francisco J. Vasconez ^{a,b,*}, Pablo Samaniego ^c, Jeremy Phillips ^a, S. Daniel Andrade ^b, Edwin Simbaña ^d, Valeria Nogales ^b, José Luis Román-Carrión ^e, Anais Vásconez Müller ^a, María Antonieta Vásquez ^f

- ^a School of Earth Sciences, University of Bristol, Bristol, Bristol, BS8 IRJ, UK
- ^b Instituto Geofísico, Escuela Politécnica Nacional, Ladrón de Guevara, E11-253, Quito, Ecuador
- ^c Laboratoire Magmas et Volcans, Université Clermont Auvergne, CNRS, IRD, OPGC, F-63000, Clermont-Ferrand, France
- ^d Sacharxeos CIA Ltda, Tulipanes 153, Sangolquí, Ecuador
- e Departamento de Biología, Facultad de Ciencias, Escuela Politécnica Nacional, Ladrón de Guevara, E11-253, Quito, Ecuador
- f Universidad San Francisco de Quito, Av. Diego de Robles & Vía Interoceánica, Quito, Ecuador

ARTICLE INFO

Keywords: Debris flow Pre-Hispanic settlements Caranqui culture Cayambe Non-volcanic Post-eruntive

ABSTRACT

In Ecuador, a country with numerous potentially active volcanoes, recurrent large earthquakes, and regular climate-related events, it is surmised that phenomena such as debris flows have affected pre-Hispanic populations since their settlement in ~5000 cal BC. Here, using a multidisciplinary approach, we studied the most recent debris flow events that affected the Cayambe city area, located 15 km west of the active glacier-clad Cayambe volcano. Based on detailed characterization of the deposits, including sedimentological, archaeological, and paleontological analyses, as well as radiocarbon dating. We found that two debris flow (i.e., Río Blanco I and II) destroyed Caranqui settlements in 665-775 cal AD and 774-892 cal AD, respectively, while another event impacted a Spanish colonial farm in 1590-1620 cal AD (Río Blanco III). The grain size distribution of these deposits indicates a gravel-rich flow for Río Blanco I and clay-rich flow for Río Blanco II and III, whilst componentry suggests low juvenile volcanic content for all three deposits. Juvenile components include pumice and lustrous dense dacites, while accidental clasts are dull dense dacites, oxidized and hydrothermally-altered material, as well as archaeological artifacts. These results, in addition to radiocarbon ages, suggest that the debris flows could either be post-eruptive or not related to volcanic eruptions. Potential non-volcanic trigger mechanisms for these events include rainfall and/or earthquakes, which implies that they can occur at any time and without forecast. Currently, the city of Cayambe is rapidly expanding and, consequently, our findings are relevant for creating impact scenarios for future debris flows forming in the Rio Blanco headwaters and descending to the city.

1. Introduction

Worldwide, human settlements have been strongly influenced by sudden geological and climate-related destructive phenomena. Multi-disciplinary approaches based on archaeology and geology have provided insights into the negative impacts produced by these natural phenomena in (pre-) historical times (e.g., Sigurdsson et al., 1982; Siebe et al., 1996; Cashman and Giordano, 2008; Bottari et al., 2009; Riede, 2016; Ugalde, 2017; Rosi et al., 2019; Riede et al., 2020). For instance, two of the most iconic and well-studied cases are Ercolano and Pompeii

towns, which were buried by pyroclastic material expelled during the paroxysmal eruption of Vesuvius volcano (Italy), back in AD 79 (Sigurdsson et al., 1982; Cioni et al., 2000). Other examples include the eruptions of Laacher See (Germany) in ~13 ka BP which affected hunter-gatherer communities in Northern Europe (Riede, 2008; Blong et al., 2018), Aira (Japan) in 30 ka BP (Smith et al., 2013), Popocatépetl (Mexico) between 800 and 215 BC and again in AD 822–823 (Siebe et al., 1996), and the explosive eruptions of Merapi (Indonesia) which destroyed Buddhist and Hindu temples back in AD 732 and 900 (Newhall et al., 2000). Moreover, other natural phenomena have been studied

^{*} Corresponding author. School of Earth Sciences, University of Bristol, Bristol, Bristol, BS8 IRJ, UK. *E-mail addresses*: fjvasconez@igepn.edu.ec, fj.vasconez@bristol.ac.uk (F.J. Vasconez).

from a multidisciplinary approach including the partial flank collapse of Stromboli (Italy) which triggered tsunamis in the Late Middle Ages (Rosi et al., 2019), destructive earthquakes in Sicily (Italy) between 400 BC and AD 600 (Bottari et al., 2009), and meteorological hazards in Britain (United Kingdom) in AD 1000–1550 (Brown, 2015).

In Ecuador, most catastrophic events are caused by volcanic or seismic activity, which results from the subduction of the Nazca plate beneath the South American plate (Gutscher et al., 1999; Witt et al., 2006; Nocquet et al., 2014, Fig. 1a). Consequently, 76 Quaternary volcanoes have been identified on the mainland (Fig. 1a); 24 are categorized as active (last eruption during the Holocene, including those that erupted after the Spanish Conquest, i.e. \sim AD 1534) and two of them are currently in eruption (Ramon et al., 2021). Additionally, based on historical seismological and marine paleo-seismological records, large earthquakes (>7.5 Mw) at the Colombian-Ecuadorian subduction margin have occurred every 40-70 years (Migeon et al., 2017) during super-cycles that lasted ~600 years and were separated by ~300 years of quiescence (Nocquet et al., 2016). Moreover, since historical times (AD 1534), there are numerous reports of cities in the Inter-Andean Valley that have been struck by shallow-crustal 5.0-7.6 Mw earthquakes related to the north-eastward motion of the North Andean Sliver (NAS, Fig. 1a) (Beauval et al., 2010, 2013). At least two large historical earthquakes have also induced landslides of volcanic terrains that then transformed into debris flows: in AD 1698 at Carihuairazo volcano (Wolf, 1873; Kolberg, 1977; Vásconez et al., 2009; Vasconez et al., 2022) and in AD 1868 at Cotacachi volcano (Stübel and Reiss, 1987). On the other hand, climate-related hazards occur constantly in Ecuador because of the combination of various factors such as: steep topography (Andean range), seasonal rainfalls, lithology, land use and cover, among others. For instance, based on newspaper articles from AD 1900-1989, Peltre (1989) created a detailed database of the climate-related events in Quito (Fig. 1a), the capital city of Ecuador. He found 517 events in 89 years, which corresponds to more than 4 damaging events per year, on average. Most recently, the largest climate-related events that have occurred in Ecuador, included the La Josefina landslide (Cuenca - AD 1993) (Zevallos et al., 1996), strong rainfall and associated floods triggered by "El Niño" phenomenon (ENSO) which affected the coastal region in AD 1997-1998 (Pourrut, 1998), the abandonment of San-Rafael waterfall (Reyes et al., 2021), which triggered an intense, still ongoing, upstream and lateral erosion of Coca river jeopardizing towns and critical infrastructure such as oil pipelines and a hydroelectric power plant (CELEC-EP, 2020; Sandoval, 2020; Jara, 2021) and the deadly La Gasca mudflow that affected the capital city in January 2022 and claimed the life of 28 people (Díaz, 2022).

Prior to the Spanish Conquest, little is known about disasters in Ecuador because of the absence of written language. However, because of the long pre-Hispanic occupational history of the Ecuadorian Andes

during the Pre-ceramic (5000-1500 cal BC; Athens, 2003), Formative (3000-500 cal BC), Regional Development (500 cal BC - 500 cal AD), Integration (500-1500 cal AD) and the Inca (AD 1500-1534) periods (Molestina, 2011; Le Pennec et al., 2013; Zeidler, 2016; Cordero, 2017), pre-Hispanic populations must have been affected by several catastrophic geological and climate-related phenomena (Knapp and Ryder, 1983; Isaacson, 1987; Hall and Mothes, 2008b). For instance, Le Pennec et al. (2013) found that a major sector collapse at Tungurahua volcano triggered a large explosive eruption, which generated a lateral blast and a Plinian eruption that devastated settlements from the Formative period in ~1100 cal BC. Hall and Mothes (2008a, 2008b) found that the enormous Chillos Valley debris flow, which originated from a sector collapse of Cotopaxi volcano in ~4500 cal BP (Mothes et al., 1998), buried soils which contained ceramics from the early Formative Period. Zeidler (2016), concluded that three volcanic eruptions disrupted the regional archaeological record and significantly affected the Jama-Coaque culture in the Formative Period. Mothes (1998) also reported that various ash fallout layers blanketed pre-Hispanic populations, such as at: "El Inga" site (Schobinger, 1988; Villalba, 1988) during the eruptions from Cotopaxi volcano in the Pre-ceramic period, Cotocollao settlements in Quito (Villalba, 1988; Molestina, 2011) during Atacazo-Ninahuilca, Cotopaxi and Pululahua eruptions in the Formative Period, and at the "La Florida" site (Molestina, 1973) during Guagua Pichincha eruptions in the Regional Development period. For the Integration Period, Molestina (2011) found evidence that Pichincha volcano debris flows affected the "Rumipamba" settlement in Quito, while Villalba and Domínguez (2009) found the ~800 BP Quilotoa's ashfall deposit (Hall and Mothes, 2008a) blanketing man-made agricultural ridges ("camellones") in the Cayambe valley. In most cases, these events had the effect of persuading pre-Hispanic population to abandon the affected areas for various years, which were later usually re-occupied (Hall and Mothes, 2008b; Zeidler, 2016).

2. Case study: the city of Cayambe

The Caranquis (Carangue/Quillaco) and Cayambis (Cayambes) nations (Espinosa Soriano, 2016; Larrain Barros, 2016b) developed in the Northern Ecuadorian Andes (Bray, 1992; Ontaneda, 2010; Espinosa Soriano, 2016) from 0.55°N to 0.15°S (Espinosa Soriano, 2016), during the second half of the Integration Period between ~950 and ~1550 cal AD (Oberem, 1981). Some communities (known as "ayllus") of these nations settled at the western and northern slopes of the glacier-capped Cayambe volcano, in the region where nowadays Cayambe county is located with a population of more than 107,000 people (Fig. 1a, INEC, 2020). To the west, the Río Blanco is the main drainage traversing the city and directly drains the glacier meltwater from the upper volcano flanks (Fig. 2). The Río Blanco valley is used for livestock grazing and

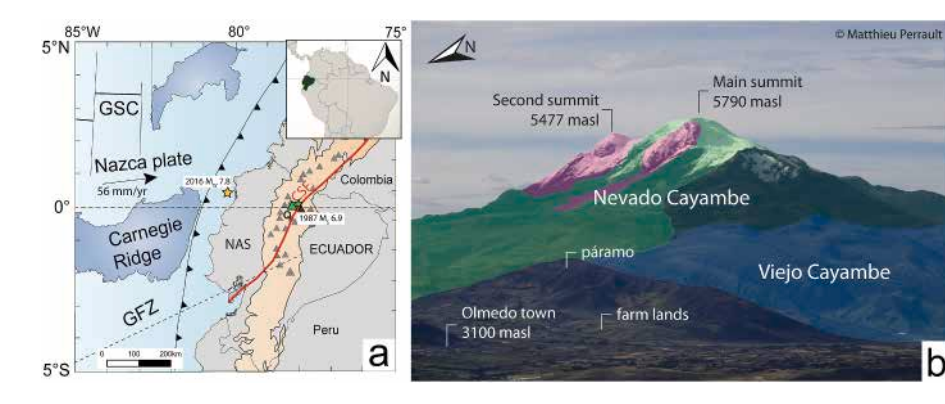


Fig. 1. a) Geodynamical setting of continental Ecuador: subduction of Nazca plate beneath the South American plate. Location of Cayambe volcanic complex shown as a green triangle and El Reventador volcano as dark brown triangle. Quaternary volcanoes as grey triangles and Andean range in light orange. Red line delimits the main transpressive right-lateral fault system, Chingual-Cosanga-Pallatanga-Puná (CCPP) system to the east of the continental North Andean Sliver (NAS), CSF: Chingual - La Sofia major Fault, Q: Quito city, GFZ: Grijalva fracture zone, GSC: Galapagos spreading centre. Orange and green stars show the epicentre of Pedernales and El Reventador earthquakes, respectively. b) Cayambe volcanic complex as seen looking towards the southeast. Viejo Cayambe is highlighted in blue, while the dark green, green and pink zones make up Nevado

Cayambe. Pink polygons depict the youngest eruptive domes towards the north and northeast emplaced in the last 4000 yr BP. Photo by M. Perrault (reproduced with permission of the author). (For interpretation of the references to colour in this figure legend, the reader is referred to the Web version of this article.)

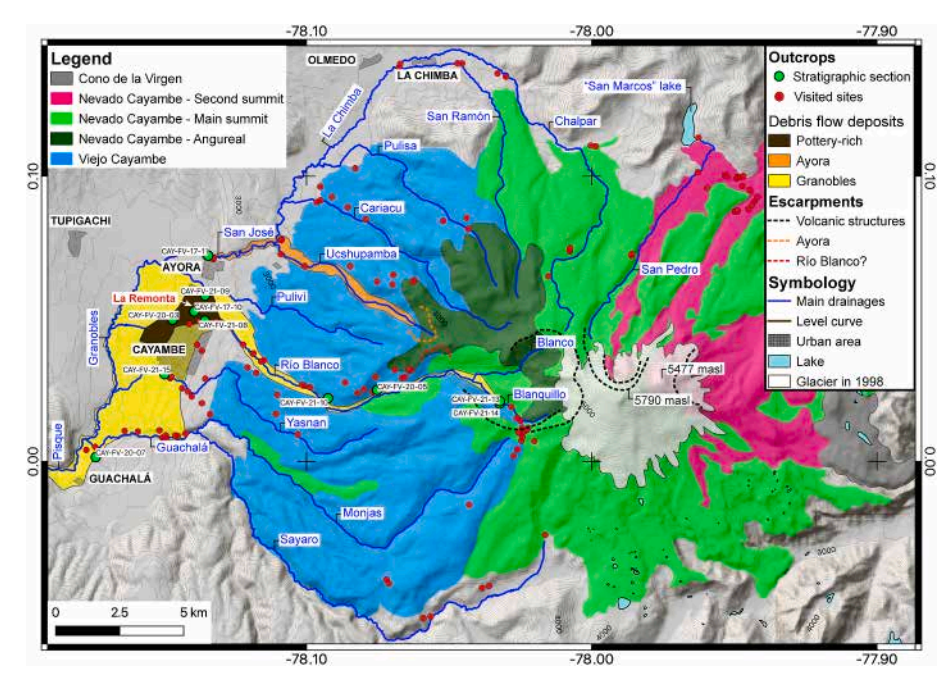


Fig. 2. a) Geological map of Cayambe volcanic complex highlighting its main eruptive stages (modified from Samaniego et al., 2005); the white polygon is the area covered by the glacier in AD 1998 (Farinotti et al., 2019). Red dots depict the sites visited, while green dots are the sites where we carried out detailed deposit descriptions and sampling. Note that the entire volcanic complex is covered by various layers of young volcanic soils interlayered with pyroclastic deposits; these were not included on this map to be able to distinguish the main underlaying geological units. (For interpretation of the references to colour in this figure legend, the reader is referred to the Web version of this article.)

agricultural tillage, mainly for flowers and traditional crops such as corn and potatoes. Over the last two decades, Cayambe city has significantly grown, expanding its urban outline, especially to the north of the Río Blanco drainage on "*La Remonta*" area (Fig. 2).

Climate-related hazards such as wildfires, droughts and local landslides have frequently affected the city of Cayambe (La Hora, 2004a, 2004b; El Comercio, 2020), although no official databases exist that catalogue these phenomena. However, studies of catastrophic natural events such as volcanic eruptions and earthquakes have been conducted because of their large potentially negative impact on local populations, as described below.

Cayambe is an active glacier-clad volcano (0.03°N, 77.98°W, 5790 masl) (Samaniego et al., 1998), located in the Cordillera Real of the Ecuadorian Andes, 15 km east of Cavambe city. Cavambe has an extensive glacier that covered 17.73 km² in AD 1998 (Jordan and Hastenrath, 1998; Farinotti et al., 2019), but since then glacier have been in retreat. Cayambe is a volcanic complex composed of two different edifices (Samaniego et al., 2005): the older one (1050-1100 ka), named Viejo Cayambe, makes up the western flank of the complex and is highly eroded and blanketed by thick (>5-10 m) successions of pyroclastic deposits interlayered with paleo-soil horizons. The younger one, named Nevado Cayambe, is a compound volcano located further to the east, (Fig. 1b). Nevado Cayambe is made up from three main structures aligned from West to East, Angureal dated by Ar-Ar at 405-413 ka, the Main summit which is younger than 230-260 ka, and the Second summit which forms the youngest Holocene edifice of the complex (Fig. 2). A small, possibly Holocene satellite vent, named "Cono de la Virgen" is located to the easternmost part of the complex (Fig. 2). According to Samaniego et al. (1998), over the last 4000 years, the volcanic activity was focused on the Main and Second Summits. They reported at least 24 eruptions during the Late Holocene separated by quiescent periods. Specially during those quiescent periods volcanic soils formed on top of the edifices under moist and cold conditions, favouring the growth of high grassland vegetation (páramos) found at altitudes between ~3500 and ~5000 m asl (Mena et al., 2001; Buytaert et al., 2006, Fig. 1b). The historical report from Ascásubi (1802) dates Cayambe's most recent eruption at AD 1785-1786. It produced limited ash fallout at Cayambe city and debris flows towards the uninhabited northern and eastern flanks. However, new historical evidence (see supplementary material 1) suggests that this eruption was indeed a long-lived event that

went on intermittently until AD 1809 (Anonymous, 1809; Hassaurek, 1868). Due to a volcanic-seismic crisis in AD 2001–2002 and based on its historical eruptive history, the Instituto Geofísico of Escuela Politécnica Nacional (IG-EPN) published the first volcanic hazard map in AD 2002 and its companion booklet in AD 2004 (Samaniego et al., 2002, 2004). The map synthetizes the most likely zones to be impacted by the most common hazardous phenomena which include ash fallout, pyroclastic currents, and volcanic debris flows (lahars). The last seismic crisis at Cayambe occurred in June 2016 (IGEPN, 2016). It began two months after the Pedernales earthquake, 7.8 Mw (Nocquet et al., 2016), which occurred 200 km west of the volcano (Fig. 1a). Recently, Butcher et al. (2021) have attributed this seismic crisis to the internal motion of hydrothermal fluids set off by the ascent of a new magma batch, which was initiated by a change in the static stresses following the Pedernales earthquake. Notably, the last volcanic eruption that affected Cayambe city was that of El Reventador volcano on 3 November 2002. The city and its surrounding farms located 56 km to the northwest of the volcano, were strongly affected by the heavy ashfalls mixed with rain, which destroyed some roofs, in particular those made of plastic used by the flower-farming companies, and polluted the drinking-water system of the city, causing significant economic losses (Hall et al., 2004).

Regarding seismic disasters affecting Cayambe area, a notable event occurred on 5 March 1987, in which two large earthquakes (6.1 and 6.9 M, Fig. 1a) associated with a segment of the Rio Chingual – La Sofia system (CSF, Fig. 1a) (Tibaldi et al., 2007; Alvarado et al., 2016), struck the areas between Cayambe and El Reventador volcanoes (Hall, 2000). Around the inhabited epicentral region, the earthquakes induced a large number of landslides, several of which evolved to debris flows (Tibaldi et al., 1995; Schuster et al., 1996). In the month preceding the earthquakes, about 600 mm of rain fell in the area, saturating the uppermost soils, which rapidly turned into highly fluidized mass-movements and debris flows after the earthquakes (Schuster et al., 1996). The vast majority of the damage was caused by mudslides which entered into major rivers and destroyed 40 km of the Trans-Ecuadorian oil pipeline as well as the only highway connecting Quito with the oil fields in the Amazonian basin (Schuster et al., 1996). The estimated bulk volume of the mass wastage ranged from 75 to 110 million m³ and the economic losses were estimated at US\$ 1 billion (Schuster et al., 1996).

Importantly, recent excavations at the north of the Río Blanco drainage, in the area where nowadays the new Cayambe city is expanding, have revealed the existence of pottery-rich volcanic breccia deposits close to the surface ("La Remonta" in Fig. 2), which are similar to those reported by Samaniego (2004). The purpose of this study is to investigate how (pre-) Hispanic cultures were affected by debris flows, using a multidisciplinary approach involving sedimentology, archaeology, and paleontology to characterize the deposits, their timing of occurrence, and finally, to provide some insights into their potential trigger mechanisms, and thus implications for future hazards.

3. Materials and methods

Data and samples of sediments, charcoals fragments, bones, and archaeological artifacts for this study were initially obtained by field-work carried out in the main drainages of the western flank of Cayambe volcano (Fig. 2). We obtained detailed geological information from the description and dating of stratigraphic sections and from granulometric and componentry analysis of key samples from volcanic breccias and fines-rich deposits. Additionally, archaeological, and paleontological analyses were carried out on pottery fragments and skeletal remains found within the volcanic breccia deposits.

3.1. Geological samples

More than 150 outcrops were visited and studied at the main drainages of the western flank of Cayambe volcano (Fig. 2). Two geological profiles were established to carry out detailed description and sampling: one longitudinal along the Río Blanco drainage, and one transversal along a North-South transect. For the sediment samples, grain size distribution (GSD) analysis based on manual sieving and a laser scattering particle size distribution analyser were performed on 12 samples. For the manual sieving, we dried the samples in an oven at 40 °C before sieving them for the range of 64 mm (-6 phi) to 0.25 mm (2phi) in one phi steps, where phi is -log₂ (diameter). The nominally sub-0.25 mm fraction was analysed in a Horiba LA-960 laser diffraction analyser at the IG-EPN. Five measurements of 0.1 g of each sample were performed to ensure reproducibility. For refractive indexes (real and imaginary), we used the dacitic composition references reported in Vogel et al. (2017) and deionized water as diluting. Both, the manual and laser granulometry were then combined assuming similar clast densities i.e., comparable weight and volume percent. In addition, we performed componentry analysis on the fractions from 64 to 0.5 mm, following the methodology presented in Eychenne et al. (2012). The clasts between 64 and 2 mm were washed manually and classified using a magnifying glass. In those fractions, all or at least 300 randomly selected clasts were classified. The fractions from 1 to 0.5 mm were washed in water and cleaned in an ultrasonic bath to remove the fine clay-coating. The cleaned grains were dried in an oven at 40 °C and at least 300 of them were later examined under a binocular microscope and classified into one of the eight component groups based on lithology, texture, and lustre. The defined component groups are: white pumice, lustrous dense dacite, dull dense dacite, volcanic glass, free crystals, oxidized material (including rhizoconcretions or root traces), hydrothermally altered grains, and archaeological fragments.

Finally, radiocarbon ages of charcoal sticks found within the deposits were carried out at the Centre of Isotope Research, Groningen University (Netherlands) and at the Laboratoire de Mesure du Carbone14 (LMC14), Saclay (France) by using an accelerator mass spectrometer (AMS) and following pre-treatment and analytical procedures described in Mook and Streurman (1983) and Dumoulin et al. (2017). Calibration of the ¹⁴C ages were performed by means of a simplified approach proposed by Talma and Vogel (1993) using Calib 8.2 (Stuiver and Reimer, 1986; Stuiver et al., 2021) and atmospheric data of the Intcal20 calibration curve (Reimer et al., 2020).

3.2. Archaeological and paleontological samples

We carried out an archaeological excavation by hand at *La Remonta site* (78.139°W, 0.053°N, 2841 masl, Fig. 2) using the technique of stratigraphic excavation in a 1×1 meter topographic grid system and 3D rendering. In addition, we collected archaeological artifacts at Puluví outcrop (78.136°W, 0.058°N, 2831 masl, Fig. 2). In both sites, we systematically collected, classified, and labelled the findings, i.e., pottery fragments and obsidian artifacts. Afterwards, the fragments were manually washed with a toothbrush and then dried at room temperature (20 °C) for 48 h. The diagnostic fragments were inventoried, drawn, and reconstructed to their original shapes based on their artifact morphology (Oberem and Wurster, 1989). In this way, we estimated the relative age of the vessels, which is assumed to be close to the occurrence date of the volcanic breccia event in which the fragments were found and identified the (pre-) Hispanic culture that they could have belonged to.

Additionally, two skeletal remains collected in one of the volcanic breccia deposits were mechanically cleaned by using dental reamers and dissecting needles. Polyvinyl acetate (Paraloid B72) dissolved in 20% thinner was used for consolidation, while polyvinyl alcohol was used as glue in the restoration process. Finally, the skeletal fragments were compared with the collection of the Paleontology Laboratory of the Department of Biology at the Faculty of Sciences of the Escuela Politécnica Nacional (EPN) to identify the corresponding specimen and taxonomic group.

4. Results

4.1. Geological mapping

Volcanic breccia deposits were identified alongside the San José, Puluví, Río Blanco, Yasnán and Guachalá rivers (Fig. 2). These deposits vary in colour, texture, sorting, thickness, sedimentological structures, GSD and componentry. The description of the two geological profiles that were established are detailed below.

4.1.1. Río Blanco longitudinal profile (A-A') - East to West

The Río Blanco river forms from the confluence of the Blanquillo and Blanco ravines at $\sim\!3750$ m asl (Fig. 3a). Río Blanco is one of the main drainages of Cayambe's glacier meltwater towards the west (Fig. 2). Its basin covers an area of $\sim\!29~{\rm km}^2$ and it is $\sim\!23~{\rm km}$ long, from the headwater to the confluence with the Granobles river (Fig. 2). The headwaters spring from a 3000 m wide W-shaped escarpment that opens towards the west (Fig. 2), with steep slopes that reach more than 300 m in relief (Fig. 3a). This escarpment resulted from a sector collapse most likely caused by hydrothermal alteration that weakened the western flank of Nevado Cayambe edifice during the Late Pleistocene (Detienne et al., 2017). As a result of this event, the steep slopes of the upper Río Blanco valley are characterized by a widespread hydrothermal alteration. Ten kilometres downstream, the basin narrows to 600 m wide and 150 m deep, while at the city level (17 km downstream, Fig. 3b), it is only 200 m wide and 3–10 m deep.

We identified 7 key outcrops along the Río Blanco profile. The most upstream one is Blanquillo I (CAY-FV-21-13) at 3854 m asl (Figs. 2 and 3b). At its base, a yellowish, poorly sorted volcanic breccia with centimetre-to meter-sized volcanic blocks is observed. It is at least 2 m-thick, but its precise depth could not be determined since its lower contact is buried (Fig. 3c). The largest blocks as well as the matrix are derived from a hydrothermally altered source zone, and the deposit description matches that provided by Detienne et al. (2017) for the Granobles cohesive debris flow which occurred at Nevado Cayambe volcano western flank in the Late Pleistocene. Cayambe city was built on top of this deposit, and we considered it as a marker layer throughout this study. The Granobles debris flow covers a minimum area of 27–30 km² (Fig. 2), and its thickness ranges from 5 to 20 m at the Cayambe plain, resulting in an estimated bulk volume of 135–600 million m³. At

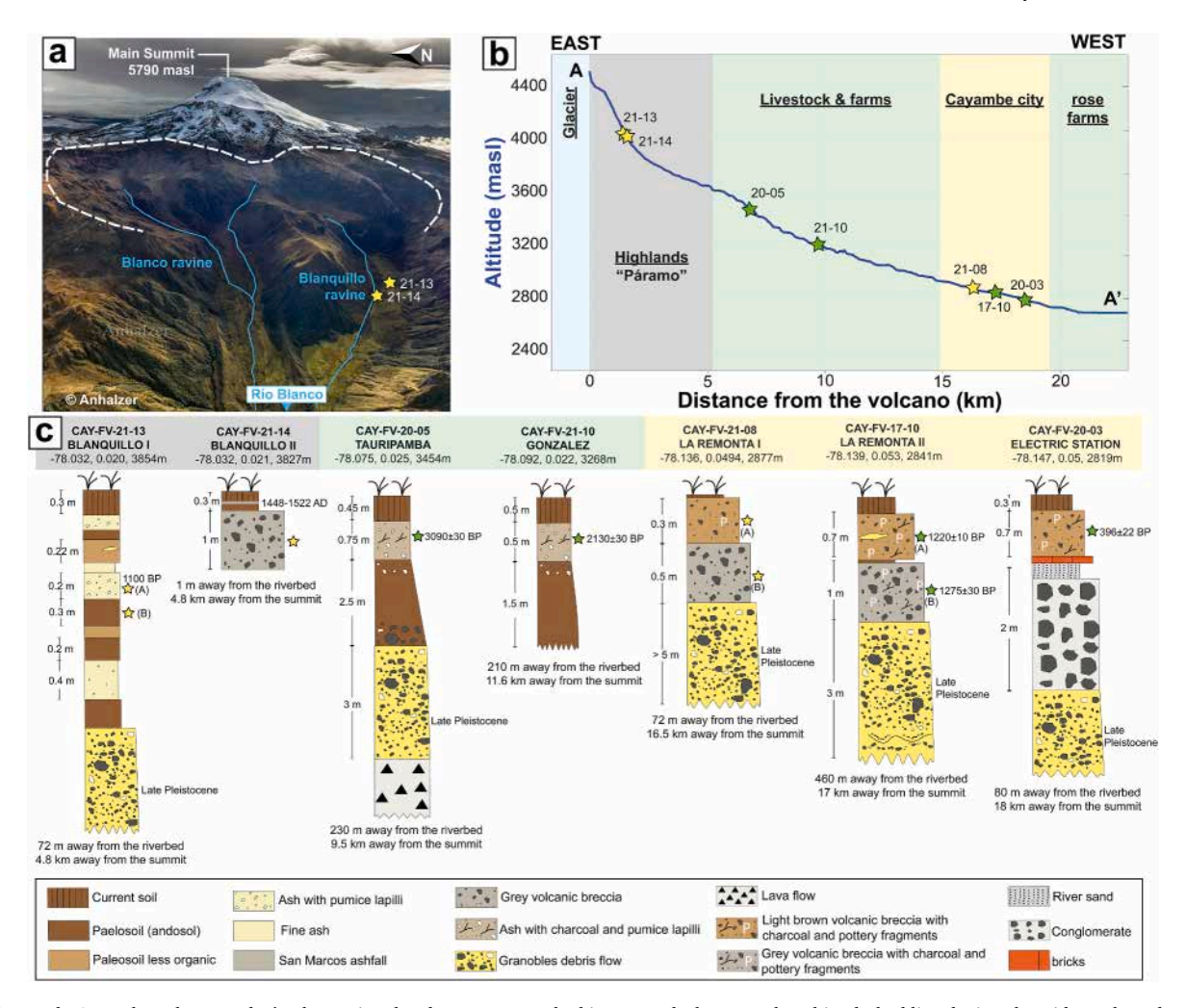


Fig. 3. a) Nevado Cayambe volcano and Río Blanco river headwaters as seen looking towards the East. The white dashed line depicts the wide W-shaped escarpment at the western headwaters of Cayambe, while the light blue lines are the main drainages. Yellow stars denote visited outcrops. Photograph by J.J. Anhalzer (reproduced with permission of the author). b) Longitudinal profile along the Río Blanco river, stars highlighting the outcrops and the different coloured backgrounds depict the current land use. c) Detailed stratigraphic sections along the Río Blanco river. Yellow stars are sampling points for GSD and componentry analysis, while green stars are sites where additionally radiocarbon dating was obtained. Note that each section has its own vertical scale. (For interpretation of the references to colour in this figure legend, the reader is referred to the Web version of this article.)

the Blanquillo I outcrop, the Granobles debris flow is overlain by a series of black and brown, 0.2–0.3 m-thick deposits, with disseminated lapilli pumice in a sand to silt-sized matrix (Fig. 3c). These darker deposits are interbedded with various 0.1–0.4 m-thick, beige to light brown alternating sand and silt layers which contain carbonized sticks and disseminated pumice lapilli clasts (Fig. 3c). Both, beige and darker deposits show signs of bioturbation including rhizoconcretions generated by roots under favourable humidity conditions (Retallack, 2001).

Blanquillo II (CAY-FV-21-14, 3827 m asl, Figs. 2 and 3b) is located 27 m lower than Blanquillo I outcrop and 1 m away from the riverbed. At the base of Blanquillo II, there is a dark grey, consolidated, poorly sorted, 1 m-thick breccia, with rounded and sub-rounded centimetre-to decimetre-large blocks, in a sand-sized and vesicle-rich matrix (Fig. 3c). This deposit is overlain by two thin, dark brown layers intercalated by a grey, thin ash layer which corresponds to an eruption at Cayambe volcano known as the San Marcos event that occurred in 1448–1522 cal AD (Vizuete, 2020). Five kilometres downstream of Blanquillo II, the Tauripamba outcrop is located at 3454 m asl (CAY-FV-20-05, Figs. 2, 3b and 3c). At its base, a massive, thick, dark grey andesitic lava flow is observed. Overlaying it is the Granobles debris flow with a thickness of 3 m (Fig. 3c). A 2.5 m-thick, dark brown layer with hydrothermally altered blocks at its base and disseminated white pumice lapilli close to its upper contact follows up the sequence. On top is a 0.75 m-thick beige

sand and silt deposit with disseminated charcoal sticks and white/yellow pumice. The charcoal yielded an age of 3090 \pm 30 BP (1424-1270 cal BC) (Table 1). This section is topped by a brown layer of 45 cm thickness. At 3268 m asl and 11.6 km away from the main summit, the Gonzalez section (CAY-FV-21-10) is made up of three thick layers (Figs. 2 and 3b), and from top to bottom these are: (i) the current soil, (ii) a light brown, sand and silt layer with disseminated pumice lapilli clast and charcoal sticks, and (iii) a similar but darker, fine-grained deposit. The charcoal in the second layer yielded an age of 2130 \pm 30 BP (204-50 cal BC) (Table 1, Fig. 3c).

The *La Remonta* I & II and the Electric Station outcrops are in the urban area of Cayambe city (Figs. 2 and 3b). *La Remonta* I (CAY-FV-21-08) is located at 2877 m asl and 72 m away from the edge of the current Río Blanco riverbed (Fig. 3c). At its base, the Granobles debris flow (>5 m) is overlain by a 0.5 m-thick grey volcanic breccia. This deposit incorporates blocks of up to 10 cm in size in a sandy matrix which exhibits vesicles (Fig. 3c). A light brown deposit with large volcanic rocks and few small pottery fragments in a sand-sized matrix follows up the sequence. At 2841 m asl and 460 m away from the edge of the current riverbed, the La Remonta II (CAY-FV-17-10) archaeological excavation has at its base the Granobles debris flow deposit, which is overlain by a 1 m-thick, grey volcanic breccia with blocks from 5 to 30 cm in diameter in a sandy matrix which contains vesicles (17-10 C). Within the latter,

Table 1
Radiocarbon ages and calibrated age conversions using IntCal20 Northern Hemisphere curve (Reimer et al., 2020) and Calib8.2 (Stuiver et al., 2021). Geographic coordinates refer to longitude, latitude and altitude in the WGS84 projection. In lab number row, SacA refers to LMC14 laboratory and GrM to Groningen University.

Outcrop, sample & (lab number)	Locality and coordinates	Sample material and deposit	δ13C (‰)	Conventional radiocarbon age (year BP $\pm\ 1\sigma)$	Calibrated age (year cal AD/BC) 68.3% (1σ)	Calibrated age (year cal AD/BC) 95.4% (2σ)
CAY-FV-20-05 (SacA 62272)	Tauripamba –78.075, 0.025, 3454	Charcoal in fines- rich deposit	-25.90	3090 ± 30	1412-1376 cal BC 1350–1302 cal BC	1424–1270 cal BC
CAY-FV-21-10 (SacA 62273)	Gonzalez –78.092, 0.022, 3268	Charcoal in fines-	-30.30	2130 ± 30	197-182 cal BC 179–101 cal BC 67-59 cal BC	346-316 cal BC 204–50 cal BC
CAY-FV-17-10 (B)	La Remonta II -78.139,	rich deposit Charcoal in volcanic breccia	-24.40	1275 ± 30	679–709 cal AD 711–748 cal AD 758–768 cal AD 771–773 cal AD	665–775 cal AD 790–822
(SacA 62277) CAY-FV-17-10 (A)	0.053, 2841 La Remonta II -78.139,	Charcoal in	-24.26	1220 ± 10	788–827 cal AD 861–863 cal AD	cal AD 773–776 cal AD 786–840
(GrM 11325) CAY-FV-20-03	0.053, 2841 Electric Station	volcanic breccia Charcoal in	-23.52	396 ± 22	1451–1490 cal AD 1604–1607 cal	cal AD 845–878 cal AD 1444–1512 cal AD
(GrM 27285) CAY-FV-21-09	-78.147, 0.050, 2819 Puluví -78.136,	volcanic breccia Charcoal in	-26.52	1189 ± 24	AD 775–777 cal AD 779–789 cal AD	1590–1620 cal AD 774–892 cal AD 931–941
(GrM 27279)	0.058, 2831	volcanic breccia			825-884 cal AD	cal AD

we found and collected various pottery fragments, obsidian artifacts (see section 4.3) and charcoal sticks which yielded an age of 1275 ± 30 BP (665–775 cal AD) (Table 1). Above this deposit, there is a 3 cm-thick, red brown, sand and silt-sized, well-consolidated, and burnt archaeological floor (Fig. 3c). On top of this paleo-floor, is a 0.7 m-thick, light brown, sand-rich deposit, with some volcanic blocks and various pottery fragments, obsidian artifacts and charcoal sticks (17-10 A, Fig. 3c). Radiocarbon analysis yielded an age of 1220 ± 10 BP (786–840 cal AD) for this deposit (Table 1). Finally, the Electric Station outcrop (CAY-FV-20-03) lies at an altitude of 2819 m asl along this longitudinal profile (Figs. 2, 3b) and 80 m away from the edge of the current riverbed. The Granobles debris flow deposit observed at the base is overlain by a series of fluvial deposits (conglomerate and sand, Fig. 3c). At this location, the fluvial deposits are covered by a row of light red bricks each 15×30 cm

in size. These are overlain by a light brown, sand-rich vesiculated deposit, with pottery fragments, obsidian artifacts and few charcoal fragments that yielded an age of 396 ± 22 BP (1444–1512 cal AD) (Table 1). Downstream of the Electrical Station outcrop, flower and livestock farms cover most of the area and no outcrops are available. Río Blanco river flows a few kilometres further west to finally join the Granobles river (Fig. 2).

4.1.2. North-South profile (B-B')

The North-South profile cuts the following main drainages at Viejo Cayambe's lower western flank from 2830 to 2720 m asl: the San José, Puluví, Río Blanco, Yasnán and Guachalá rivers, when viewed from north to south (Figs. 2 and 4a). Volcanic breccia deposits were identified in all of them and are described below (Fig. 4).

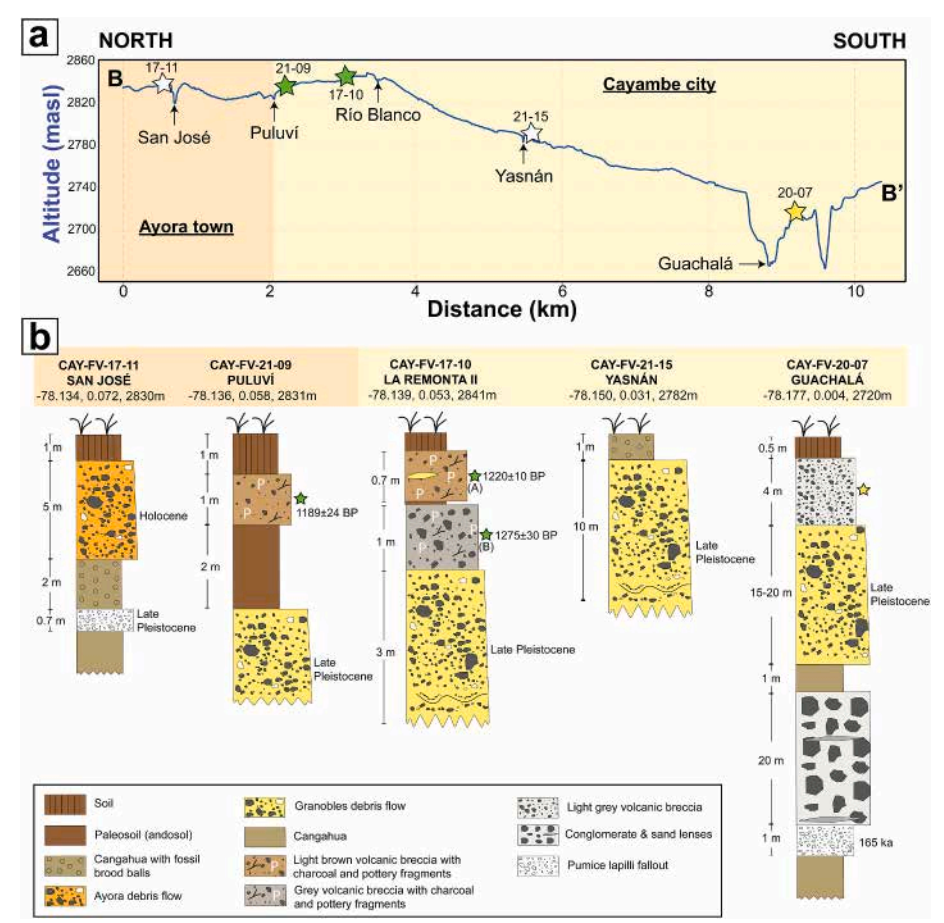


Fig. 4. a) North-South cross-section along the main drainages of Cayambe volcanic complex at the lower western flank, from North to South: The San José, Puluví, Río Blanco, Yasnán and Guachalá rivers. White stars are visited points, yellow stars are sampling sites where GSD and componentry analyses were carried out, while green stars are outcrops where in addition radiometric dating was performed. b) Detailed stratigraphic sections along the main drainages of Cayambe volcano. Notice that each section has its own vertical scale. (For interpretation of the references to colour in this figure legend, the reader is referred to the Web version of this article.)

The San José outcrop (CAY-FV-17-11) lies at 2830 m asl, at the right margin of the river and to the north of Ayora town (Figs. 2, 4a and 4b). At the base, a light brown, sand-silt-sized, indurated, mostly reworked volcanic deposit, locally known as Cangahua is observed, it formed between ~500 and 10 ka (Winckell and Zebrowski, 1992; Hall and Mothes, 1997). Interbedded with Cangahua, there is a 0.70 m-thick, pumice lapilli fall deposit corresponding to a rhyolitic fallout from Lower Fuya-Fuya which occurred in the Late Pleistocene (Robin et al., 2009; Bablon et al., 2020). Above this pumice fall deposit, an overlying Cangahua layer shows fossil brood balls, related to the activity of dung beetles, and probably large herbivores (dung suppliers), that formed under long, interglacial and fluctuating syn-eruptive conditions during the Late Pleistocene (Sánchez et al., 2013). On top of the Cangahua, a yellowish, poorly sorted, 5 m-thick volcanic breccia with centimetre-to meter-sized blocks in a sand-sized matrix is observed. This breccia was previously identified by Detienne et al. (2017) as the Ayora debris flow, which occurred in the Holocene due to a high-altitude mass movement of volcanic soils (>3200 m asl). Detienne et al. (2017) suggested that the source of the Ayora and Granobles debris flows lies in the headwaters of the Río Blanco river. However, based on our detailed mapping of several outcrops, we found that the Ayora debris flow initiated upstream of Ucshupamba ravine (~4000 m asl) in the upper flanks of *Viejo Cayambe* edifice (orange dashed line in Fig. 2). The Ayora debris flow deposit covers a minimum area of 3–4 km² and its thickness ranges from 5 to 10 m, yielding an approximated bulk volume of 15–40 million m³, which is one order of magnitude smaller than that of Granobles (135-600 million m³). At this location, the Ayora debris flow deposit is covered only by the present-day soil (Fig. 4b).

The Puluví outcrop (CAY-FV-21-09) is located 2831 m asl to the south of Ayora town (Figs. 2 and 3b). The Granobles debris flow is found at its base, above which is a 2 m-thick black layer, comprised of sand-to silt-sized grains and is well-sorted and massive. Overlaying it is a 1 mthick, light brown, sand-rich, vesicular matrix deposit, with some volcanic rocks a few centimetres to decimetres in size, and pottery fragments, obsidian artifacts and charcoal sticks (Fig. 4b). Various pottery fragments and two skeletal remains were collected from this deposit for further analyses (see section 4.3). The charcoal sticks yielded an age of 1189 ± 24 BP (774–892 cal AD) (Table 1). Based on the observed deposits, the Puluví outcrop marks the northernmost lateral run-out distance of both, the Granobles and the pottery-rich breccia deposits (Fig. 2). The latter initiated in the Río Blanco and covers a minimum area of $\sim 3 \text{ km}^2$ with thicknesses from 0.5 to 1 m at Cayambe city, vielding an approximate bulk volume of $\sim 1.5-3$ million m³ - one and two orders of magnitude smaller than the Ayora and Granobles debris flow deposits, respectively. At Yasnán outcrop (CAY-FV-21-15, 2782 m asl) a ~10 m-thick Granobles debris flow deposit is overlain by Cangahua with fossil brood balls, as observed at the CAY-FV-17-11 outcrop (Fig. 4b). Finally, the Guachalá outcrop (CAY-FV-20-07) is made up of various meters of Cangahua interbedded with a 1 m-thick, white pumice lapilli fallout which originated at Chacana caldera between 180 and 200 ka (Bigazzi et al., 1992) or ~165 ka (Hall and Mothes, 1997), and a thick (20 m) series of grey fluvial deposits (conglomerate and sand) (Fig. 4b). On top of the Cangahua outcrops a 15-20 m-thick section of the Granobles debris flow. At its top, a light grey, 4 m-thick, moderately sorted, massive, clast-supported deposit is observed containing many dense lustrous dacites from 2 to 15 cm in size. The present-day soil covers the entire stratigraphic section (Fig. 4b).

4.2. Grain size distribution (GSD) and componentry proportions

GSD and componentry analyses were performed on 12 key samples from the two previously mentioned profiles (Figs. 2, 3c and 4b). They include eight volcanic breccias and four fines-rich deposits. The Granobles and Ayora debris flow deposits were not included in this analysis because they have already been studied in detail by Detienne et al. (2017) and the present investigation focuses on Holocene events.

Note that CAY-FV, the prefix for all samples, is omitted for brevity in the following detailed sample descriptions.

4.2.1. Volcanic breccia deposits

The volcanic breccia samples were clustered into five main deposits based on stratigraphic position, lithofacies criteria and age (radiometric, when available). From the oldest to the youngest these are: Guachalá, Río Blanco I, II, III and IV.

- i) *Guachalá deposit (sample 20-07*, Fig. 2): Its GSD is unimodal around 4 mm, it is moderately sorted (2 phi), and its median lies between 4 and 8 mm (Fig. 5a). It is clast-supported, with gravel making up 81 wt%, while the remaining 19 wt% correspond to matrix (i.e., sand + silt + clay material, Fig. 5a). Most of its components are lustrous dense dacite (45.6%), while 21.1% are dull dense dacites, 16.4% are hydrothermally altered and 13.4% oxidized material. Pumice, free crystals, and volcanic glass add up to 3.4% of the component proportions (Fig. 5b).
- ii) Río Blanco I deposit (samples 21-08 B and 17-10 B): Sample 21-08 B was collected upstream of the La Remonta II site (Fig. 2). It has four modes at 0.0078, 0.25, 8 and 64 mm, and, thus, is very poorly sorted (5 phi), with its median lying between 8 and 16 mm (Fig. 5a). It is clast supported (70 wt% > 2 mm) and most of its components are oxidized clasts (45.2%), dull dense dacites (38.9%) and hydrothermally altered material (11.3%). The remainder (4.6%) is made up of lustrous dense dacite (1.6%), volcanic glass (1.3%), free crystals (1%), pumice (0.6%) and archaeological fragments (0.1%) (Fig. 5b). Sample 17-10 B was taken at the La Remonta II site (Fig. 2). It has three modes at 0.0078, 0.25 and 8 mm. It is very poorly sorted (5 phi), and its median lies between 2 and 4 mm (Fig. 5a). It is clast supported (57 wt% > 2 mm) and almost half of its components are oxidized (46.9%), followed by hydrothermally altered material (33.9%) and dull dense dacites (10.9%). The remaining components are lustrous dense dacites (3.8%), pumice (1.8%), free crystals (1.2%), volcanic glass (0.9%) and archaeological artifacts (0.6%) (Fig. 5b). Importantly, the observed GSD and componentry trends from upstream (21-08 B) to downstream (17-10 B) indicate that the Río Blanco I event deposited large clasts upstream, while it incorporated archaeological artifacts downstream (Figs. 2 and
- iii) Río Blanco II deposit (samples 21-08 A, 17-10 A and 21-09, Fig. 2): Sample 21-08 A, which lies furthest upstream of these three outcrops (Fig. 3b), has four modes at 0.016, 0.063, 0.25 and 4 mm and is poorly sorted (4 phi). Its median lies between 0.063 and 0.125 mm (Fig. 5a) and it is matrix-supported (82 wt% < 2 mm). Dull dense dacites make up 30.4% of its clasts, while oxidized (23.3%), hydrothermally altered (22.3%) and lustrous dense dacites (11.2%) comprise together the highest component proportions (Fig. 5b). The remaining material (12.8%) corresponds to archaeological fragments (5%), volcanic glass (3.7%), free crystals (2.7%) and pumice (1.4%). Sample 17-10 A at the La Remonta site has three modes at 0.0078, 0.125 and 32 mm. It is very poorly sorted (5.5 phi), its median lies between 0.125 and 0.25 mm (Fig. 5a), and it is matrix-supported (65 wt% < 2 mm). Based on componentry analysis it is made up of 69.5% dull dense dacites, 8.1% hydrothermally altered and 6.5% oxidized clasts, 5.8% of archaeological fragments and 5.5% lustrous dense dacites. The remaining material (4.6%) is volcanic glass, free crystals, and pumice (Fig. 5b). Finally, sample 21-09 is located the furthest downstream and it represents the northern edge of this deposit. It has three modes at 0.0078, 0.25 and 16 mm. It is very poorly sorted (5 phi), and its median lies between 0.5 and 1 mm. It is supported by 57 wt% of sand, silt, and clay (Fig. 5a) and most of its clasts are archaeological fragments (37.8%), oxidized clast (25.2%), dull dense dacites (11.1%), hydrothermally altered

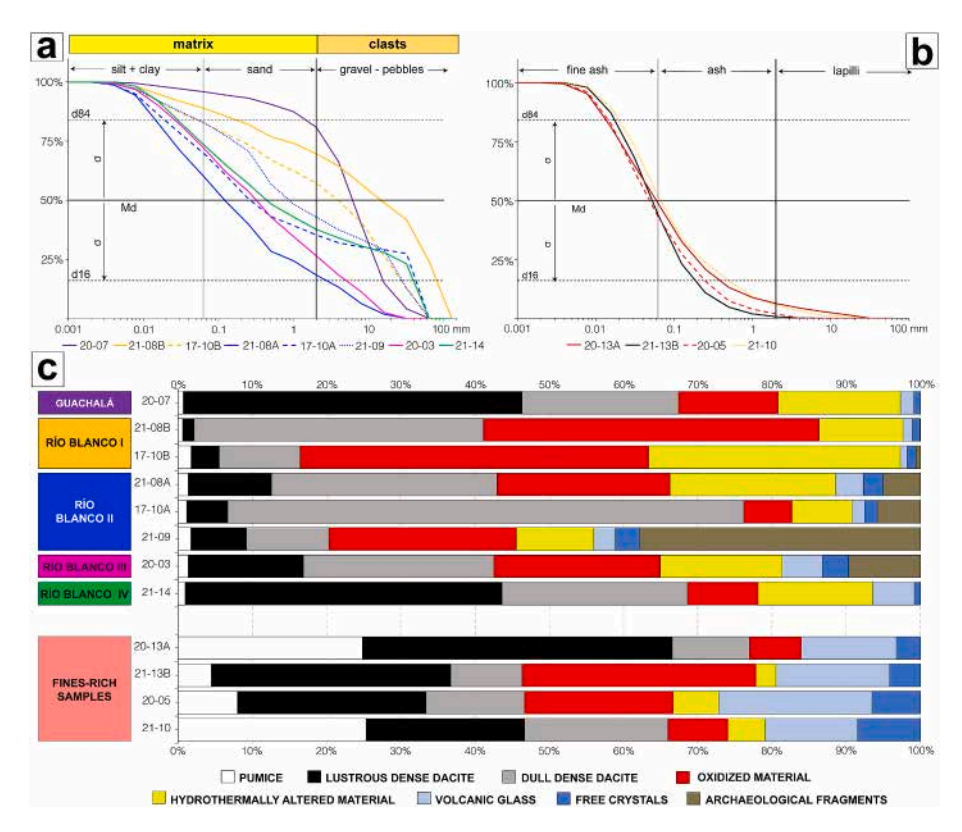


Fig. 5. Cumulative grain size distribution of a) eight volcanic breccias b) four fine-rich deposits. The black solid line at 50% indicates the median (Md) and the dashed lines at 16 and 84% the standard deviation (σ). Sand or ash(<2 mm) and silt or fine ash (<63 μ m) are plotted for reference, respectively. The different line colours refer to the various deposits: Guachalá (purple), Río Blanco I (orange), Río Blanco II (blue), Río Blanco III (magenta), Río Blanco IV (green), and fines-rich samples (black, dark red, red, and orange). The different line style highlights the location of the sample along the river as follows: solid line (upstream), dashed line (midway) and dotted line (downstream). c) Componentry of eight volcanic breccias and four fines-rich samples for the combined size fractions between 0.5- and 64-mm. The component types are shown in the legend. (For interpretation of the references to colour in this figure legend, the reader is referred to the Web version of this article.)

material (10.5%) and lustrous dense dacites (7.5%) (Fig. 5b). The remaining 7.9% are made up of free crystals (3.3%), volcanic glass (2.9%) and pumice (1.7%). Interestingly, the GSD analysis reveals that this deposit incorporated large clasts downstream, which is also reflected in the significant increase in archaeological fragments from 5% to 37.8% (Fig. 5b).

- iv) Río Blanco III deposit (sample 20-03, Fig. 2): This outcrop is the lowest one of those analysed along the Río Blanco profile (Fig. 3b). It has three modes at 0.063, 0.25 and 8 mm, it is very poorly sorted (4.5 phi), and its median lies between 0.25 and 0.5 mm (Fig. 5a). It is matrix-supported (73%) and its main components are 25.6% dull dense dacites, 22.4% oxidized clast, 16.4% hydrothermally altered material, 15.5% lustrous dense dacites and 9.7% archaeological fragments (Fig. 5b). The remaining material (10.4%) is made up of volcanic glass (5.5%), free crystals (3.5%) and pumice (1.4%).
- v) Río Blanco IV deposit (sample 21-14, Fig. 2): Located at the headwaters of the Río Blanco river (Fig. 3a), it has two modes at 0.016 and 32 mm and is very poorly sorted (6 phi), with its median lying between 0.25 and 0.5 mm (Fig. 5a). It is matrix-supported (62 wt%) and most of its clasts are lustrous dense dacites (42.7%), followed by 25% dull dense dacites, 15.4% hydrothermally altered material and 9.5% oxidized clasts (Fig. 5b) which include rhizoconcretions. The remaining percent (7.4%) is made up of volcanic glass (5.6%), pumice (1%) and free crystals (0.8%).

Summarizing, the Guachalá and Río Blanco IV deposits are enriched in lustrous dense dacite (42.7–45.6%), which indicate a high juvenile contribution, while their different GSDs possibly reflect the different flow dynamics during deposition at the sites where the samples were taken, at different distance from the source (Fig. 2). Based on field descriptions and the classification scheme proposed by Scott et al. (1995), Guachalá is a hyperconcentrated flow while Río Blanco IV is a granular debris flow, at the sampled locations. In contrast, the Río Blanco I, II and

III deposits are rich in accidental clasts (74–95%) and poor in juvenile material (1.6–15.5%). Accidental clasts include the sum of dull dense dacites (<69.5%), oxidized (<46.9%) and hydrothermally altered material (<33.9%), as well as archaeological fragments (<37.8%). Additionally, differences in GSD are observed and possibly highlight varying flow dynamics, even though distances from the source are similar for the three deposits (Fig. 2). Río Blanco I is clast supported and matches a granular debris flow deposit, while Río Blanco II and III deposits are matrix supported and akin to clay-rich debris flows. These three deposits, which occurred between 1275 and 396 BP, incorporated archaeological fragments as well as charcoal sticks.

4.2.2. Fines-rich deposits

All fines-rich deposits are bioturbated and contain rhizoconcretions as described below. Deposit colour varies from beige to dark brown (Figs. 2 and 3b), which likely depends on the degree of weathering (i.e., secondary mineralization) and organic carbon content.

- i) The beige *sample 21-13 A* (Fig. 2) has a main mode at 0.063 mm, it is poorly sorted (3 phi) and fine-grained (Md between 0.031 and 0.063 mm, Fig. 5c). It is matrix-supported (94 wt%) and comprises 41.7% lustrous dense dacite, 24.9% pumice, 12.8% volcanic glass, and 10.4% dull dense dacites. The remaining 10.3% is made up of oxidized material (7%) and free crystals (3.3%) (Fig. 5b).
- ii) The dark brown *sample 21-13 B* (Fig. 2) is unimodal at 0.031 mm, moderately sorted (2 phi), its median lies between 0.031 and 0.063 mm (Fig. 5c), and it is matrix-supported (99 wt%). Its main components are lustrous dense dacite (32.2%), oxidized material which include rhizoconcretions (31.5%) and volcanic glass (15.3%). Minor percentages of dull dense dacites (9.6%), pumice (4.5%), free crystals (4.2%) and hydrothermally altered material (2.7%) are also included (Fig. 5b).
- iii) The light brown *sample 20-05* (Fig. 2) shows a main mode at 0.016 mm, is poorly sorted (2.5 phi) and its median lies between

0.031 and 0.063 mm (Fig. 5c). It is also matrix-supported (98 wt %) and its main components are lustrous dense dacite (25.4%), volcanic glass (20.7%), oxidized material which include rhizoconcretions (20%) and dull dense dacites (13.3%). The remained is made up of pumice (8%), free crystals (6.5%) and hydrothermally altered material (6.1%) (Fig. 5b).

iv) The dark brown *sample 21-10* (Fig. 2) is unimodal at 0.031 mm and poorly sorted (2.5 phi). Its median lies between 0.063 and 0.125 mm (Fig. 5c) and it is matrix-supported (94 wt%). Its main components are pumice (25.3%), lustrous dense dacites (21.4%), dull dense dacites (19.3%) and volcanic glass (12.5%). The remaining material includes free crystals (8.5%), oxidized material (8.1%) which include rhizoconcretions, and hydrothermally altered clasts (5%) (Fig. 5b).

4.3. Archaeological and paleontological analyses

4.3.1. Archaeological results

Most of the collected archaeological artifacts are pottery fragments from 50 to 150 mm in length with wall thicknesses between 3 and 20 mm. In few cases, the fragments are very thin (3–5 mm), light and feature a red slip glaze. Vessels of this type have been found along the valleys of the Northern Ecuadorian Andes (from the border with Colombia to 2° S) and belonged to the Cosanga (Panzaleo) culture that developed during the Regional Development and the Integration Period, i.e. from \sim 500 cal BC to \sim AD 1500 (Jijón y Caamaño, 1997; Ontaneda, 2002). Additionally, obsidian artifacts (Fig. 6a) collected at these sites constitute evidences of pre-historic trade activities (Gratuze, 1999) and/or domestic use. Most of the pottery fragments, however, have thick walls (>10 mm), are smooth and discoloured (i.e. undecorated) and have soot patterns and oxidation patches, which are typically observed on cooking vessels (Hally, 1983; Skibo, 1992). Most of these fragments

once made up different parts of vessels, such as bodies and necks. In few cases, they correspond to rims, which are diagnostic fragments used to identify and restore the vessels to their original shape.

Here, we describe three diagnostic rims in detail, one from the Río Blanco I deposit (17-10 B) at La Remonta II excavation site (Figs. 2 and 3b), two from the Río Blanco II deposit at La Remonta II and Puluví outcrops (17-10 A and 21-09) (Fig. 4b) and one from the Electric Station outcrop (Fig. 3c):

- i) Diagnostic fragment from the Río Blanco I deposit (17-10B, Fig. 6b). The fragment is 76 mm long (Fig. 6c) and 6-8 mm-thick with smooth internal and external surfaces. The fabric contains ~0.5 mm large inclusions of pumice, quartz, feldspars, micas, and clay pellets; the latter being a typical feature of recycled raw material probably originating from broken or discarded vessels (Peacock, 1977). The surface, margins and core are reddish-brown, 2.5 YR 5/4 on the Munsell scale, which is a colour system for the recording of pottery colour by hue, value and chroma (Orton and Hughes, 2013). Same colour on both, margins and core, indicates long and oxidizing firing conditions in the kiln during elaboration (Orton and Hughes, 2013). On its external surface, the fragment has a soot coating suggesting that it was probably used for cooking. The diagnostic fragment matches the description of Oberem and Wurster (1989) for Caranqui phase I type G vessels (Fig. 6c).
- ii) Diagnostic fragments from the Río Blanco II deposit: At Puluví outcrop we found a triangular-shaped fragment of 71 mm in length, 66 mm in width (Fig. 6d) and 6–8 mm in thickness. Its exterior and interior surfaces are smooth, and its fabric is 2.5 YR 5/6 red at the margins and core which is in agreement with long oxidizing firing (Orton and Hughes, 2013). The paste contains inclusions of ~0.5 mm in diameter of pumice, quartz, feldspars

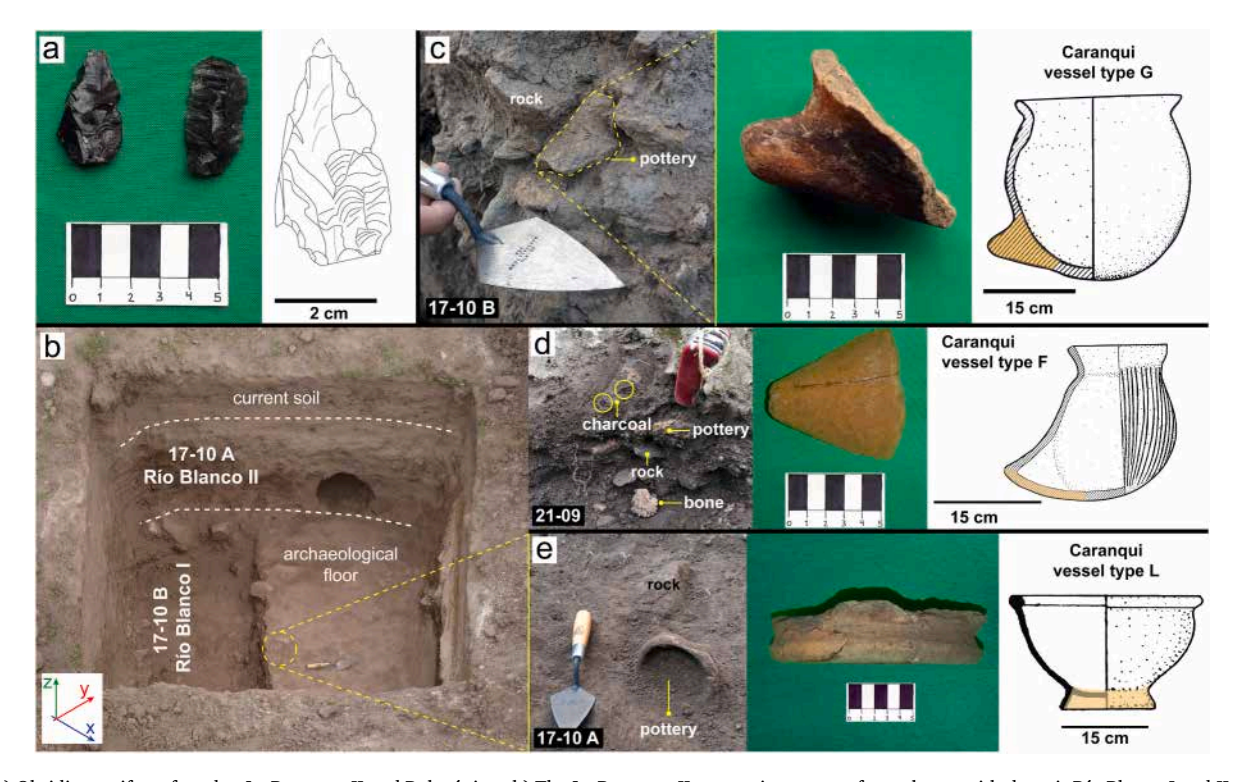


Fig. 6. a) Obsidian artifacts found at La Remonta II and Puluví sites, b) The La Remonta II excavation as seen from above, with deposit Río Blanco I and II separated by an archaeological floor. Diagnostic rims from left to right (c–e): picture of the fragment within the deposit, picture after cleaning and sketch of how the vessel looked like in its original shape. c) diagnostic rim at the Río Blanco I deposit, sample 17-10B, d) diagnostic rim at the Río Blanco II deposit, sample 21-09, e) diagnostic rim at the Río Blanco II deposit, sample 17-10A. Note that the orange shadow in the sketch depicts the corresponding fragment recovered from the deposit. Vessel types according to Oberem and Wurster (1989). (For interpretation of the references to colour in this figure legend, the reader is referred to the Web version of this article.)

and micas, and clay pellets ~2 mm in diameter. This fragment does not have soot patterns suggesting that it probably broke soon after being made and fell into disuse. This fragment matches with Caranqui phase I type F vessels (Fig. 6d) reported by Oberem and Wurster (1989). At the La Remonta II site (Fig. 6b), in sample 17-10A, we found an annular base fragment (Fig. 6e). It is circular, 132 mm in diameter and its wall thickness varies between 8 and 11 mm. It has a smooth external surface and a rough internal wall. Its fabric contains inclusions of ~ 0.5 mm diameter of pumice, quartz, feldspars, micas, and clay pellets. The core is diffuse and dark grey because of incomplete burning of organic carbon in the raw material (Orton and Hughes, 2013), while the external margins are reddish-brown (2.5 YR 4/4) suggesting that the mouth of the pot was closed (i.e., reductive environment) (Orton and Hughes, 2013). This matches the description of Carangui phase I type L vessels in Oberem and Wurster (1989) (Fig. 6e).

iii) Additionally, we found a row of bricks below the Río Blanco III deposit (Fig. 3c). Each brick is rectangular-shaped and 300 mm long, 150 mm wide and 50 mm-thick. It has a rough external surface and its fabric is 2.5 YR 6/8 light red at the margins and core which is in agreement with long oxidizing firing (Orton and Hughes, 2013). Bricks were not made during pre-Hispanic times, but they began to appear after the Spanish Conquest in around AD 1534. Therefore, the row of bricks could possibly correspond to vestiges of a Spanish colonial farm that was inundated by the Río Blanco III event.

Summarizing, throughout Río Blanco I and II deposits, obsidian artifacts can be found suggesting trade activities (Gratuze, 1999) and/or domestic use. Moreover, all the observed pottery fragments were broken and had charcoal fragments around them. The analysis of the diagnostic pottery fragments concluded that they belong to the pre-Hispanic Caranqui culture, phase I, which developed from at least 950 cal AD to AD 1550 (Oberem, 1981; Oberem and Wurster, 1989). In most cases, fragments are undecorated, their walls are smooth and thick, and have soot patterns, suggesting that they were mainly of domestic use. This is supported by the abundance of charcoal sticks nearby, which also indicates they were used for cooking. However, some fragments are very thin and have a red slip glaze. These characteristics match vessels made and used in the same area by the Cosanga culture, which developed between 500 cal BC - AD 1500 (Jijón y Caamaño, 1997; Ontaneda, 2002). From the archaeological evidence, we conclude that these two debris flow events occurred between 500 BC and AD 1550, and most likely between AD 950 and 1500. Additionally, the row of bricks found below Rio Blanco III deposit at the Electric Station outcrop (Fig. 3c) suggests that this event occurred during colonial times (i.e., after AD 1534), which is roughly in agreement with the second peak radiocarbon age of 1590-1620 cal AD (Table 1).

4.3.2. Paleontological results

Two skeletal remains were found together at the Puluví outcrop (Fig. 4b) within the Río Blanco II deposit that was dated at 774–892 cal AD (Table 1). The first fragment (Fig. 7a) is 5 cm long (x), 2 cm wide (y) and 5 cm high (z). It has one molar and four premolar teeth and constitutes a part of an upper maxilla. The second one is 5 cm long, 3.5 cm wide and 3 cm high and corresponds to a distal extremity of a left tibia (Fig. 7b). Based on a comparison of the dental formula (i.e. I 1/3, C 1/1, P 2/1, M 3/3), we identified that the maxilla fragment belongs to species Lama glama (Mammalia, Artiodactyla, Camelidae) (Linnaeus, 1758; Nowak, 1999; Tirira, 2007). Moreover, using the existing sample collection of the paleontology laboratory form the EPN, we found that the tibia also belongs to a Lama sp.

Llamas are found in the páramo and Inter-Andean scrubland ecosystems of the Northern Andes. They have been domesticated for thousands of years (6–7 ky) and are considered excellent pack animals





Fig. 7. Skeletal animal remains belonging to Lama sp. a) Fragment of upper maxilla seen from lateral view (xz plane) and occlusal view (xy plane), b) distal extremity of a left tibia from the lower view (xy plane). Note that z axis (height) points to the zenith.

(Tirira, 2007). From the paleontological analysis, we conclude that llamas lived together with the affected pre-Hispanic settlements, in particular during the Río Blanco II event. Although, this finding did not provide any additional age constraints, this information implies that llamas have been domesticated in the Cayambe area at the time of the event occurrence.

5. Discussion

5.1. Deposits interpretation and potential trigger mechanism(s)

Most of the deposits that blanket Cayambe volcanic complex originated from the last 4 ky of eruptive activity of Nevado Cayambe (i.e., primary and reworked ash-rich volcanic deposits). This activity was clustered into three main eruptive cycles which lasted ~200–1000 years each, separated by quiescent periods of 600–1000 years (Samaniego et al., 1998). Some of these ash-rich volcanic deposits transformed into volcanic soils due to moist and cold weather conditions at páramo altitudes (Zehetner et al., 2003; Delmelle et al., 2015), especially during repose periods even though it is a continuous process. At first sight, the brown colour (i.e., organic carbon content), the fines-rich material, disseminated pumice lapilli and the absence of sedimentary structures (dunes and/or ripples) of the analysed fines-rich deposits led us to

interpret them as reworked volcanic deposits or even organic-poor soil horizons. However, the presence of charcoal sticks, the high percent of juvenile material (Fig. 5c) and its thickness variations between valley bottom and interfluves were key features to identify their eruptive origin. In this context, charcoal indicated that the deposits must have been hot during emplacement and most likely correspond to dilute pyroclastic currents, which served as a parent material for the formation of volcanic soils before being buried by younger deposits. Therefore, deposits 20-05, 21-10 and 21-13A (Fig. 3c) are considered diluted pyroclastic current deposits, which depict the most recent eruptive activity (i.e., between 3090 and 1000 BP) of Nevado Cayambe towards the Río Blanco valley. On the other hand, deposit 21-13B (Fig. 3c) correspond to a volcanic soil depicting a quiescent period. Both, diluted pyroclastic current deposits and volcanic soils, are similar regarding their grain size distribution (Fig. 3b) and componentry (Fig. 3c), but vary in the deposit colour and charcoal fragments content.

Cayambe city has grown and expanded on top of the Río Blanco alluvial fan, which is largely made up by the huge Granobles debris flow deposit (Fig. 2) that probably occurred during the Late Pleistocene (Detienne et al., 2017). On top of Granobles, we found two recent deposits (Río Blanco I and II), which both contain charcoal sticks and vessel fragments. At first sight, the charcoal suggested that the deposits were hot during emplacement. However, soot patterns and oxidation patches on the external walls of the fragments of vessels suggest that they resulted from their use for cooking rather than from the hot emplacement of the flows. Charcoal fragments yielded an age of 665-775 cal AD and 774-892 cal AD, while vessels indicate that they belong to the Caranqui culture, which developed at least since 950 cal AD (Oberem, 1981; Oberem and Wurster, 1989). Therefore, our findings suggested that this culture had already settled in this area earlier than previously reported. Moreover, based on stratigraphy (Fig. 3c), GSD analysis (Fig. 5a) and radiometric calibration (Fig. 8), we verified that these deposits correspond to two different events which occurred within a relatively narrow timespan, separated only by few decades (Fig. 8). Both have high percentages of non-juvenile material (74-95 vol%)

which include dull dense dacites, archaeological artifacts, oxidized and hydrothermally altered clasts (Fig. 5c). The hydrothermally altered grains were possibly incorporated through erosive processes of the underlying deposit (i.e., Granobles debris flow) during the debris flow transit, however, mineralogical analyses on the debris flow matrix are needed for confirmation. Based on componentry and the fact that the radiometric ages match with quiescent periods of Cayambe volcano (Fig. 8), we suggest that Rio Blanco I and II are most likely eruption unrelated events and their source locations are likely on the páramo soils some kilometres downstream (~7–8 km) from the Nevado Cayambe main summit (red dashed line in Fig. 2).

In contrast, the Río Blanco III debris flow was emplaced either in 1444-1512 cal AD or 1590-1620 cal AD, depending of the chosen calibration curve peak (Fig. 8), simultaneously with the Cayambe eruptive period "San Marcos", dated at 1454–1594 cal AD (Fig. 8) (Samaniego et al., 1998; Vizuete, 2020). The San Marcos period probably lasted several decades, as reported by Céspedes in AD 1573 in Espinosa Soriano (2016) and by Sancho Paz Ponce de Leon in AD 1582 in Gómez Rendón (2016) (see red dashed lines in Fig. 8) and produced a paroxysmal event that formed San Marcos Lake to the north of the Cavambe volcano (Fig. 2). There is no stratigraphic evidence of the San Marcos eruptions affecting the lowlands of Río Blanco valley, nor historical reports of the paroxysmal event (Samaniego et al., 1998). Both suggest either limited impact of the eruption on the colonial farms settled since AD ~1539 (Municipal de Quito, 1934; Larrain Barros, 2016a) (green dashed line in Fig. 8), or that the Spanish had not yet colonized the area and therefore would not have witnessed the paroxysmal eruption. However, light red bricks were found below the Río Blanco III deposit (Fig. 3c), and since bricks were first made in Ecuador only after the Spanish Conquest, the Río Blanco III debris flow event most likely occurred after AD ~1539 and therefore during the last stage of the San Marcos eruptive period. This interpretation is in agreement with the second radiometric calibrated peak at 1590-1620 cal AD (Fig. 8). Additionally, the grain size distribution and components of this deposit are similar to those observed for the eruption unrelated Río

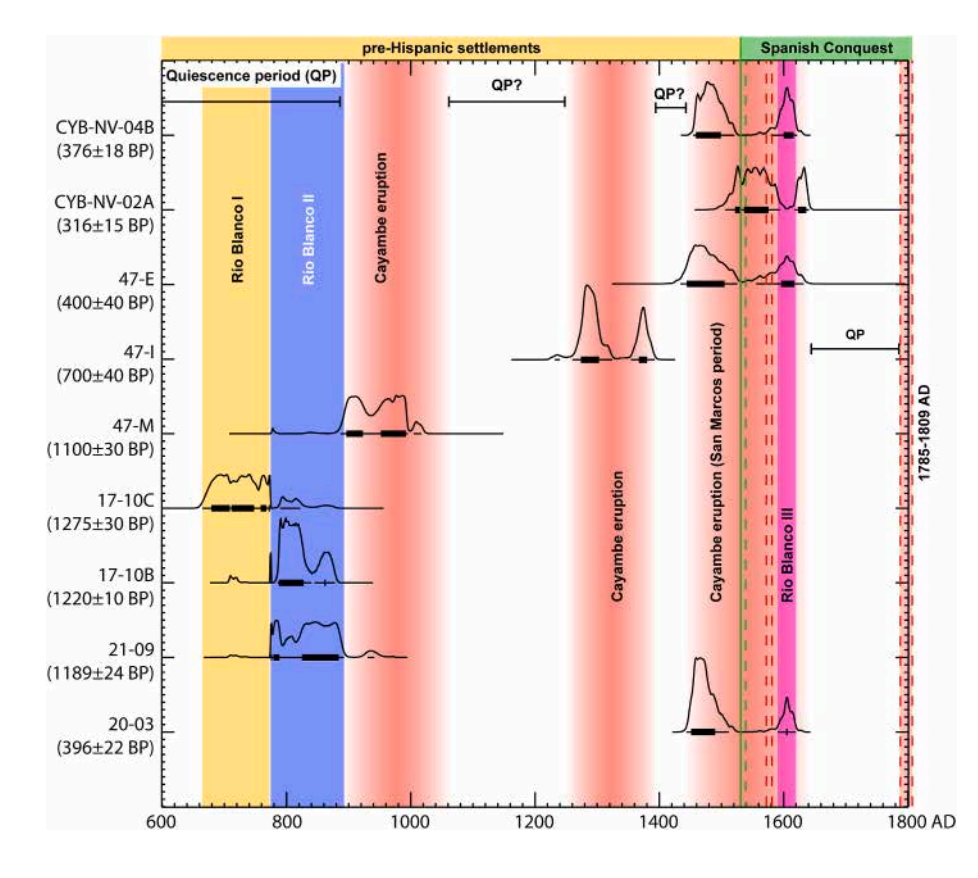


Fig. 8. Probability distribution of the calibrated radiometric dates from the debris flow events and volcanic eruptions of Cayambe volcano during the past 600 cal AD, based on Table 1, Samaniego et al. (1998) and Vizuete (2020) and using Calib 8.2 (Stuiver et al., 2021). Note that the background colours highlight the most likely occurrence period for pyroclastic currents (red) and debris flows (orange, blue and magenta). The red backgrounds were blurred at the edges to emphasize the uncertainty of the eruptive periods. The green line denotes the arrival of the Spanish to Ecuador (AD 1534) while the green dashed line denotes the establishment of the first Spanish farm close to the Río Blanco river in AD 1539 (Municipal de Quito, 1934; Larrain Barros, 2016a). Red dashed lines denote historical reports of Cayambe eruptions in AD 1573 (Espinosa Soriano, 2016), 1582 (Gómez Rendón, 2016), 1785 (Ascásubi, 1802) and 1809 (Anonymous, 1809). (For interpretation of the references to colour in this figure legend, the reader is referred to the Web version of this article.)

Blanco II deposit (Fig. 5b) suggesting that Río Blanco III is most likely a post-eruptive event. It is important to note that an earthquake (6.4 $\rm M_{IC}$) occurred in the north of Quito in AD 1587 (Fermín Cevallos, 1886; Beauval et al., 2010) which also produced damage in the Cayambe region and therefore could have been a possible trigger mechanism for initiating the Rio Blanco III event.

At Guachalá river (Fig. 2), we observed a clast-supported, massive, 5-m-thick debris flow deposit containing abundant juvenile clasts with more than 45 vol% of lustrous dense dacites. This deposit could be associated with a lava dome collapse that turned into a debris flow due to the interaction of the hot block-and-ash avalanche with the glacier (i. e., syn-eruptive debris flow or primary lahar). It occurred long after the Granobles debris flow (Fig. 4b) and is the only evidence of primary lahars that we found at the western flank of Cayambe volcano since the Late Pleistocene. Based on componentry and GSD, none of the previously described debris flow deposits resemble the Guachalá deposit, supporting our interpretation that the Río Blanco I, II and III debris flow deposits are likely eruption unrelated or post-eruptive events.

Given the stratigraphic and laboratory evidence and our interpretations, we consider other potential trigger mechanisms for the most recent pottery-rich Cayambe debris flow deposits (Río Blanco I, II and III) including rainfall and/or earthquakes, both of which are commonly invoked as mass movement triggers that eventually evolve into debris flow events (e.g. Wolf, 1873; Stübel and Reiss, 1987; Schuster et al., 1996; Basile et al., 2003; Coviello et al., 2021). Because Cayambe is located in a seismically active region (Hall, 2000; Beauval et al., 2010; Alvarado et al., 2016), it is plausible that an earthquake could have destabilized the saturated volcanic soils on the medium and high flanks of the Cayambe edifice, as has been reported for other cases worldwide (Keefer, 1984; Bommer and Rodríguez, 2002; Basile et al., 2003; Coviello et al., 2021). This could result in the formation of multiple landslides that then evolved to debris flows, as was observed to occur recently in the El Reventador - Cayambe area in AD 1987 (Schuster et al., 1996) and probably in the Early Holocene, to initiate the Ayora debris flow (Detienne et al., 2017). Our evidence then suggests that the debris flows that affected the Río Blanco valley since the Holocene, were large enough to have left a deposit (geological record), were originated by mass movements triggered perhaps by rainfall or earthquakes instead of volcanic eruptions, which is a common default interpretation for these types of deposits when found at active volcanic areas. This means that similar debris flows can occur given the appropriate trigger and without an ongoing eruptive process. These non-eruptive debris flows, at the moment are not considered in the Cayambe volcano hazard maps.

Importantly, the mineralogy of the deposits is unknown, so if they contained allophanes as a secondary soil phase, these could have caused a high level of microaggregation, which, in turn, could have skewed the GSD analysis (Churchman and Lowe, 2012). Moreover, drying clay mineral-rich soils increases this problem (Kubota, 1972; Shoji et al., 1993), so future studies of soil mineralogy should be undertaken to address these issues to prevent any bias in GSD. However, given that the volcanic ash soils from the norther Ecuadorian Andes (including Cayambe) are relatively young and poorly developed (Zehetner et al., 2003), the bias, if present, is likely to be minor. Detailed mineralogical analysis of the debris flow matrix could also provide better insights into their origin and source locations as suggested by Detienne et al. (2017). Such analyses are out of the scope of this manuscript but should be addressed in future work.

5.2. Reconstruction of the pre-Hispanic settlement and current situation of Cayambe city

Little is known about the pre-Hispanic settlements in the northern Ecuadorian Andes, mostly because the written record started around \sim AD 1534 with the Spanish conquest, but also because the Caranqui culture (Cayambi and Caranqui nations) was truncated after a war with the Incas that lasted 17–20 years, until \sim AD 1515 (Espinosa Soriano,

2016; Larrain Barros, 2016a, 2016b). This conflict ended with the massacre of Yahuarcocha, (yahuar = blood and cocha = lake, in the local quechua language), a lake 35 km north of Cayambe city, where more than 20,000 people were killed by Huayna Capac, the Inca king (González Suárez, 1904; Espinosa Soriano, 2016; Gómez Rendón, 2016). Thus, the Cayambi and Caranqui populations were drastically reduced not only by the men and women killed in that war, but also due to their subsequent deportation by the Incas to diminish their forces (Espinosa Soriano, 2016; Gómez Rendón, 2016; Larrain Barros, 2016b). Two decades later, when Sebastián de Benalcázar, one of the first Spanish conquerors, arrived, he found only small villages in the lands where once two main nations were located and thus the remaining culture was disregarded by the Spanish (Gómez Rendón, 2016). On the contrary, the neighbouring Sarance nation (Otavalo) with more than 10,000 people was extolled and therefore colonized (Gómez Rendón, 2016).

Espinosa Soriano (2016) studied in detail the Carangui and Cayambi nations using ethnohistoric methods. Here we summarize some of his most important findings about this culture during the XVI century in order to understand how the people affected by the debris flows most likely lived in the VIII and IX centuries. According to Espinosa Soriano (2016), each nation was governed by a king (Cacique, Cappacuraca or Ango) and was made up by various villages (ayllus), each with their own leader (curaca). Nations and villages were linked by blood ties, but sometimes two nations became one when there was an external threat, as was the case with the Inca invasion, when the Cayambi and Caranqui nations joined forces. Each village (ayllu) had large areas to farm and were often distributed in various ecological altitudes to take advantage of the different microclimates to produce several types of crops. Ayllus were located between 5 and 20 km away from one another, separated by artificial and natural barriers such as ravines, rivers and/or hills. They usually cultivated corn, potatoes, and quinoa and kept llamas and guinea pigs. Llamas were used as pack animals and as sacrifices, for instance, when a Cacique's house was inaugurated. Caranquis and Cayambis were farmers and lived in East-West aligned mud-thatched houses (mud and grass mix) without windows. Their cookware was made with clay in a kiln and was used in wood stoves.

Our investigation shows that two debris flows (Río Blanco I and II) destroyed pre-Hispanic settlements located close to the Río Blanco river. They occurred in a narrow timespan during the VIII and IX centuries (Fig. 8). Despite the damage produced by the Río Blanco I event, the Caranguis did not permanently abandon their settlement, on the contrary, they re-occupied it, and were then affected again by the Rio Blanco II event. The need to maintain livelihoods, the strategic location of the settlements, or simply the communities' attachment to place are reasons why re-occupation may have occurred. These are significant factors in acceptance of risk from natural hazards in modern society (Eiser et al., 2012), and may have been equally important in pre-Hispanic societies. We speculate that the later settlement affected by the Rio Blanco II event was larger than that before Rio Blanco I, as the percentage of pottery fragments of Río Blanco I is lower than the Río Blanco II deposit. Perhaps the enlargement of this settlement reflects the acceptance of risk or loss of memory of the Rio Blanco event, since its affectation was local (i.e., limited area) and discrete (i.e., no recurrent event). However, we lack evidence to make any definitive interpretation, noting instead that the inferred re-occupation of the Rio Blanco river is observed in a wide range of cultural and historical settings (Siebe et al., 1996; Hall and Mothes, 2008b; Zeidler, 2016).

Since the end of the XXth century, Cayambe city has significantly grown because of substantial national and foreign investments in rose farming. In 1998–2000, the city's growth was unplanned and informal. As an example, the northern part of the Río Blanco riverbed was filled with land fill, and the river was pushed to the south of its natural path (Fig. 9a). On top of the land fill many houses were constructed and most of them were rented to national and foreign migrants that arrived looking for job opportunities. Nowadays, six neighbourhoods are officially settled along the Río Blanco riverside, inhabited by ~ 1000 people



Fig. 9. The Río Blanco river within Cayambe city, photograph by Carlos Vasconez (reproduced with permission of the author), a) the Río Blanco river as seen looking upstream. Note that houses are on top of land fill inside the northern natural channel of the river. Nevado Cayambe volcano can be seen in the background. b) Cross-section of the Río Blanco river (North-South), orange dashed line depicts the Granobles debris flow deposit, on top of this the Río Blanco deposits I, II and III are found. The red dashed line is the overtopping level of the current channel. The black dashed arrows highlight the most likely depth differences of the terraces based on the geological record. The grey bar shows the location of infrastructure closest to the river. Note that vertical scale was exaggerated to highlight altitude differences. (For interpretation of the references to colour in this figure legend, the reader is referred to the Web version of this article.)



including locals and seasonal migrants. There are also three high schools, one elementary school, a retirement home, national and international dairy companies and more than 150 ha of rose farming located close to the river. In addition, to the north of the Río Blanco, a park, new houses, and governmental infrastructure have been constructed (Figs. 2 and 9b). In the past, Río Blanco events I, II and III most likely inundated the northern area of the alluvial fan, possibly because the northern riverside was lower than the southern one at the time (Fig. 9b). Presently it is the opposite, thus, based on the current topography of the Río Blanco alluvial fan, the southern riverside is the most prone to be inundated if a future debris flow overtops the current channel. Consequently, in the case of debris flow events of similar size, or even smaller, than those that occurred in the VIII, IX and XVI centuries, a large population and infrastructure could be affected. This means that the old city of Cayambe, which is the most inhabited part, could be significantly impacted (Fig. 9b). Because many houses are built on top of the natural channel of the river (Fig. 9a), future studies should: i) estimate the volume of the least voluminous debris flow that could produce damage, and ii) carry out a proper analysis of the soil properties (physic-chemical, hydraulic and mechanical) to test the conditions that might lead to mass movements and consequently identify the source areas of future potential slope failure/debris flow initiation.

6. Conclusions

This study presents new evidence of the threat posed by debris flows in the recent past-since the VII century, in the area where the city of Cayambe is located. Pottery fragments, skeletal remains and charcoal sticks found within three debris flows deposits indicate that pre-

Hispanic settlements from the Caranqui culture - phase I were affected by such events in 665–775 cal AD (Río Blanco I), 774–892 cal AD (Río Blanco II) and in 1590–1620 cal AD a Spanish colonial farm was inundated (Río Blanco III).

Based on granulometry, Río Blanco I deposit corresponds to a gravelrich debris flow while Río Blanco II and III are clay-rich flows. Moreover, the three deposits are poor in juvenile volcanic material, i.e., have a low content of pumice and lustrous dense dacites. Furthermore, radiocarbon dating suggests that the events occurred during quiescence periods or after eruptions. These results indicate the three Río Blanco debris flow events most likely are eruption unrelated or post-eruptive. We suggest that rainfall and/or earthquakes are plausible trigger mechanisms for such events, suggesting that they can occur at any time without forecast, given the right conditions in the source area.

At the western drainages of Cayambe volcanic complex, there is little evidence of recent debris flows (<Holocene). The few deposits large enough to have left a geological record are most likely related to mass movements in a cascade effect context. The low number of debris flow events at the western flank is possibly related to the lack of recent loose volcanic material deposition on this flank, since most of the recent eruptions of Cayambe volcano instead affected the northern and eastern flanks.

Based on radiocarbon ages obtained from charcoal sticks and the pottery fragments collected within the Río Blanco I and II deposits, we suggest that Caranqui - phase I culture is older than previous reports, i. e., 665–775 cal AD instead of 950 cal AD.

Fines-rich deposits with charcoal fragments are probably diluted and distal pyroclastic current deposits which depict the most recent eruptive activity of Nevado Cayambe towards the Río Blanco valley that occurred

between 3090 and 1000 BP.

The findings of this study are highly valuable to assess the local hazard and risk as they describe previously unknown impact scenarios that could develop downstream in the Río Blanco and other rivers. In particular, taking into account the current topography, the southern area of the Rio Blanco alluvial fan, i.e., the most inhabited part of Cayambe city, is the most likely to be affected in the case of future debris flows.

Author contributions

Conceptualization, methodology, fieldwork, formal analysis, and original draft preparation, FJV., PS., JP. and DA.; methodology and field data curation, FJV., VN. and AVM.; archaeological data curation, FJV. and ES.; paleontological data curation JLRC.; archaic analysis FJV. and MAV. All authors revised the manuscript and approved the final version.

Funding

This work was supported by the UKRI GCRF under grant NE/ S009000/1, Tomorrow's Cities Hub.

Data availability

Supporting information can be found alongside the online version of this manuscript. Supplementary material 1: Historical reports.

Declaration of competing interest

The authors declare that they have no known competing financial interests or personal relationships that could have appeared to influence the work reported in this paper.

Acknowledgments

The authors thank Gobierno Autónomo Descentralizado Intercultural y Plurinacional del Municipio de Cayambe, in particular to Agustín Quishpe (risk management technician) and MSc. Guillermo Churuchumbi (Mayor of the city) for their help and facilities during fieldwork. We also thank the late Francisco Méndez (risk management chief and city councillor of Cayambe) for his friendship and support during fieldwork. A special acknowledgment goes to Carlos Vasconez and Daniel Sierra for their selfless help. We also thank M. Perrault, J.J. Anhalzer and C. Vasconez for sharing the photos used in Figs. 1, 3 and 9, respectively. Claus Siebe, Pierre Delmelle, and an anonymous reviewer are kindly acknowledged for their thoughtful comments that improved the manuscript.

Appendix A. Supplementary data

Supplementary data to this article can be found online at https://doi.org/10.1016/j.quaint.2022.06.006.

References

- Alvarado, A., Audin, L., Nocquet, J.M., Jaillard, E., Mothes, P., Jarrín, P., Segovia, M., Rolandone, F., Cisneros, D., 2016. Partitioning of oblique convergence in the Northern Andes subduction zone: migration history and the present-day boundary of the North Andean Sliver in Ecuador: Eastern limit of the north Andean sliver. Tectonics 35, 1048–1065. https://doi.org/10.1002/2016TC004117.
- Anonymous, 1809. Breve relacion de la erupción de fuego de la montaña y Volcán de Cayambe, que observó distintamente de la galería de su casa el que la escribe.
- Ascásubi, J.J., 1802. Letter to Baron Alexander von Humboldt. Alexander von Humboldt. Athens, J., 2003. Inventory of Earthen Mound Sites, Northern Highland Ecuador.

 Honululu: Publicaciones INPC
- Bablon, M., Quidelleur, X., Samaniego, P., Le Pennec, J.-L., Santamaría, S., Liorzou, C., Hidalgo, S., Eschbach, B., 2020. Volcanic history reconstruction in northern Ecuador: insights for eruptive and erosion rates on the whole Ecuadorian arc. Bull. Volcanol. 82, 11. https://doi.org/10.1007/s00445-019-1346-1.

- Basile, A., Mele, G., Terribile, F., 2003. Soil hydraulic behaviour of a selected benchmark soil involved in the landslide of Sarno 1998. Geoderma 117, 331–346. https://doi. org/10.1016/S0016-7061(03)00132-0.
- Beauval, C., Yepes, H., Bakun, W.H., Egred, J., Alvarado, A., Singaucho, J.-C., 2010. Locations and magnitudes of historical earthquakes in the Sierra of Ecuador (1587-1996). Geophys. J. Int. https://doi.org/10.1111/j.1365-246X.2010.04569.x.
- Beauval, C., Yepes, H., Palacios, P., Segovia, M., Alvarado, A., Font, Y., Aguilar, J., Troncoso, L., Vaca, S., 2013. An earthquake catalog for seismic hazard assessment in Ecuador. Bull. Seismol. Soc. Am. 103, 773–786. https://doi.org/10.1785/ 0120120270
- Bigazzi, G., Coltelli, M., Hadler, N.J.C., Araya, A.M.O., Oddone, M., Salazar, E., 1992. Obsidian-bearing lava flows and pre-Columbian artifacts from the Ecuadorian Andes: first new multidisciplinary data. J. S. Am. Earth Sci. 6, 21–32. https://doi.org/ 10.1016/0895-9811(92)90014-P.
- Blong, R.J., Riede, F., Chen, Q., 2018. A fuzzy logic methodology for assessing the resilience of past communities to tephra fall: a Laacher See eruption 13,000 year BP case. Volcanica 1, 63–84. https://doi.org/10.30909/vol.01.01.6384.
- Bommer, J.J., Rodríguez, C.E., 2002. Earthquake-induced landslides in Central America. Eng. Geol. 63, 189–220. https://doi.org/10.1016/S0013-7952(01)00081-3.
- Bottari, C., Stiros, S.C., Teramo, A., 2009. Archaeological evidence for destructive earthquakes in Sicily between 400 B.C. and A.D. 600. Geoarchaeology 24, 147–175. https://doi.org/10.1002/gea.20260.
- Bray, T.L., 1992. Archaeological survey in northern highland Ecuador: Inca imperialism and the País Caranqui. World Archaeol. 24, 218–233. https://doi.org/10.1080/ 00438243 1992 9980204
- Brown, P.J., 2015. Adverse Weather Conditions in Medieval Britain: an Archaeological Assessment of the Impact of Meteorological Hazards (Thesis). Durham, UK.
- Butcher, S., Bell, A.F., Hernandez, S., Ruiz, M., 2021. Evolution of seismicity during a stalled episode of reawakening at Cayambe volcano, Ecuador. Front. Earth Sci. 9, 680865 https://doi.org/10.3389/feart.2021.680865.
- Buytaert, W., Deckers, J., Wyseure, G., 2006. Description and classification of nonallophanic Andosols in south Ecuadorian alpine grasslands (páramo). Geomorphology 73, 207–221. https://doi.org/10.1016/j.geomorph.2005.06.012.
- Cashman, K.V., Giordano, G., 2008. Volcanoes and human history. J. Volcanol. Geoth. Res. 176, 325–329. https://doi.org/10.1016/j.jvolgeores.2008.01.036.
- CELEC-EP, 2020. CELEC EP contratará estudios y obras de estabilización en el cauce del río Coca [WWW Document]. URL. https://www.celec.gob.ec/hidroagoyan/index.ph p/sala-de-prensa/noticias/531-celec-ep-contratara-estudios-y-obras-de-estabilizac ion-en-el-cauce-del-rio-coca, 11.9.21.
- Churchman, G.J., Lowe, D.J., 2012. Alteration, Formation, and Occurrence of Minerals in Soils. CRC press. New Zeland.
- Cioni, R., Gurioli, L., Sbrana, A., Vougioukalakis, G., 2000. Precursory phenomena and destructive events related to the Late Bronze Age Minoan (Thera, Greece) and AD 79 (Vesuvius, Italy) Plinian eruptions; inferences from the stratigraphy in the archaeological areas, 171. Geological Society, London, Special Publications, pp. 123–141. https://doi.org/10.1144/GSL.SP.2000.171.01.11.
- Cordero, M.A., 2017. Volcanismo y la búsqueda de sitios arqueológicos tempranos en el área del lago San Pablo, Sierra Norte del Ecuador. In: Volcanes, cenizas y ocupaciones antiguas en perspectiva geoarqueológica en América Latina, Estudios de Antropología y Arqueología. Centro de Publicaciones Pontificia Universidad Católica del Ecuador, Quito, Ecuador, pp. 102–114.
- Coviello, V., Capra, L., Norini, G., Dávila, N., Ferrés, D., Márquez-Ramírez, V.H., Pico, E., 2021. Earthquake-induced debris flows at Popocatépetl volcano, Mexico. Earth Surf. Dyn. 9, 393–412. https://doi.org/10.5194/esurf-9-393-2021.
- Delmelle, P., Opfergelt, S., Cornelis, J.-T., Ping, C.-L., 2015. Volcanic soils. In: The Encyclopedia of Volcanoes. Elsevier, pp. 1253–1264.
- Detienne, M., Delmelle, P., Guevara, A., Samaniego, P., Opfergelt, S., Mothes, P.A., 2017. Contrasting origin of two clay-rich debris flows at Cayambe Volcanic Complex, Ecuador. Bull. Volcanol. 79 https://doi.org/10.1007/s00445-017-1111-2.
- Díaz, V., 2022. COE de Quito eleva a 28 la cifra de víctimas del aluvión [WWW Document]. El Comercio. URL. https://www.elcomercio.com/actualidad/quito/coe-cifra-victimas-aluvion-heridos.html, 2.7.22.
- Dumoulin, J.P., Comby-Zerbino, C., Delqué-Količ, E., Moreau, C., Caffy, I., Hain, S., Perron, M., Thellier, B., Setti, V., Berthier, B., 2017. Status report on sample preparation protocols developed at the LMC14 Laboratory, Saclay, France: from sample collection to 14C AMS measurement. Radiocarbon 59, 713–726. https://doi. org/10.1017/RDC.2016.116.
- Eiser, J.R., Bostrom, A., Burton, I., Johnston, D.M., McClure, J., Paton, D., van der Pligt, J., White, M.P., 2012. Risk interpretation and action: a conceptual framework for responses to natural hazards. Int. J. Disaster Risk Reduc. 1, 5–16. https://doi.org/ 10.1016/j.ijdrr.2012.05.002.
- El Comercio, 2020. El cantón Cayambe, en el norte de Pichincha, enfrenta seis incendios forestales [WWW Document]. El Comercio. URL. https://www.elcomercio.com/act ualidad/ecuador/canton-cayambe-pichincha-incendios-forestales.html, 12.16.21.
- Espinosa Soriano, W., 2016. Cayambes y Carangues: el testimonio de la Etnohistoria. Biblioteca Cincuentenario IOA - Plutarco Cisneros Andrade, Otavalo, Ecuador
- Eychenne, J., Le Pennec, J.-L., Troncoso, L., Gouhier, M., Nedelec, J.-M., 2012. Causes and consequences of bimodal grain-size distribution of tephra fall deposited during the August 2006 Tungurahua eruption (Ecuador). Bull. Volcanol. 74, 187–205. https://doi.org/10.1007/s00445-011-0517-5.
- Farinotti, D., Huss, M., Fürst, J.J., Landmann, J., Machguth, H., Maussion, F., Pandit, A., 2019. A consensus estimate for the ice thickness distribution of all glaciers on Earth. Nat. Geosci. 12, 168–173. https://doi.org/10.1038/s41561-019-0300-3.
- Fermín Cevallos, P., 1886. Terremotos y erupciones volcánicas que han ocurrido. In: Resumen de la Historia del Ecuador desde su origen hasta 1845. Imprenta de la Nación, Guayaquil, Ecuador, p. 294.

- Gómez Rendón, J., 2016. Viajes y viajeros en la región de Otavalo. In: Biblioteca Cincuentenario IOA - Plutarco Cisneros Andrade, first ed. Instituto Otavaleño de Antropología, Otavalo, Ecuador.
- González Suárez, F., 1904. Prehistoria Ecuatorina ligeras reflexiones sobre las razas, que poblaban antiguamente el territorio actual de la República del Ecuador. Biblioteca Nacional del Ecuador "Eugenio Espejo, Quito, Ecuador.
- Gratuze, B., 1999. Obsidian characterization by laser ablation ICP-MS and its application to prehistoric trade in the Mediterranean and the Near East: sources and distribution of obsidian within the Aegean and Anatolia. J. Archaeol. Sci. 26, 869–881. https:// doi.org/10.1006/jasc.1999.0459.
- Gutscher, M.-A., Malavieille, J., Lallemand, S., Collot, J.-Y., 1999. Tectonic segmentation of the north andean margin: impact of the carnegie ridge collision. Earth Planet Sci. Lett. 168, 255–270. https://doi.org/10.1016/S0012-821X(99)00060-6.
- Hall, M., 2000. Los terremotos del Ecuador del 5 de Marzo del 1987, Deslizamientos y sus efectos socioeconómicos. Corporación Editora Nacional, Quito, Ecuador
- Hall, M.L., Mothes, P.A., 1997. El origen y la edad de la Cangahua superior, valle de Tumbaco (Ecuador). In: Suelos Volcánicos Endurecidos. Simposio Internacional, pp. 19–28.
- Hall, M.L., Mothes, P.A., 2008a. Quilotoa volcano—Ecuador: an overview of young dacitic volcanism in a lake-filled caldera. J. Volcanol. Geoth. Res. 176, 44–55. https://doi.org/10.1016/j.jvolgeores.2008.01.025.
- Hall, M.L., Mothes, P.A., 2008b. Volcanic impediments in the progressive development of pre-Columbian civilizations in the Ecuadorian Andes. J. Volcanol. Geoth. Res. 176, 344–355. https://doi.org/10.1016/j.jvolgeores.2008.01.039.
- Hall, M., Ramon, P., Mothes, P., LePennec, J.L., Garcia, A., Samaniego, P., Yepes, H., 2004. Volcanic eruptions with little warning: the case of volcán reventador's surprise November 3, 2002 eruption, Ecuador. Revista geológica de Chile 31, 349–358. https://doi.org/10.4067/S0716-02082004000200010.
- Hally, D.J., 1983. The interpretive potential of pottery from domestic contexts. Midcont. J. Archaeol. 8, 163–196.
- Hassaurek, F., 1868. Four Years Among Spanish-Americans. In: Hurd and Houghton, 459. Broome Street, New York, USA.
- IGEPN, 2016. Special report Nº1, Cayambe: Anomalía en la actividad sísmica [WWW Document]. URL. https://www.igepn.edu.ec/servicios/noticias/1351-informe-especial-volcan-cayambe-n-1-2016.
- INEC, 2020. Proyección de la población Ecuatoriana, por anos calendario, según cantones 2010-2020 [WWW Document]. Instituto Nacional de Estadística y Censos. URL. https://www.ecuadorencifras.gob.ec/proyecciones-poblacionales/, 7.25.20.
- Isaacson, J.S., 1987. Volcanic Activity and Human Occupation of the Northern Andes: the Application of Tephrostratigraphic Techniques to the Problem of Human Settlement in the Western Montaña during the Ecuadorian Formative (PhD Thesis). University of Illinois at Urbana-Champaign, USA.
- Jara, M., 2021. Obras para que Coca Codo no salga de operación tardarán hasta tres años, pero la erosión llegará antes [WWW Document]. El Comercio. URL. https://www.elcomercio.com/actualidad/negocios/obras-coca-codo-operacion-erosion.html, 11.9.21.
- Jijón y Caamaño, J., 1997. Antropología prehispánica del Ecuador, first ed. Abya-Yala, Ouito. Ecuador.
- Jordan, E., Hastenrath, S.L., 1998. Glaciers of South America: Glaciers of Ecuador. US Geological Survey professional paper.
- Keefer, D.K., 1984. Landslides caused by earthquakes. GSA Bulletin 95, 406–421. https://doi.org/10.1130/0016-7606(1984)95. & lt;406:LCBE& gt;2.0.CO;2.
- Knapp, G., Ryder, R., 1983. Aspects of the Origin, Morphology and Function of Ridged Fields in the Quito Altiplano, Ecuador. Institute of Latin American Studies, the University of Texas at Austin.
- Kolberg, J., 1977. Hacia el Ecuador: (Nach Ecuador): relatos de viaje. Traducido de la IV edicion alemana por F. Yepez Arboleda, Cuarta, Alemania 1807. In: República Federal de Alemania y Pontificia Universidad Catolica del Ecuador, Quito, Ecuador.
- Kubota, T., 1972. Aggregate-formation of allophanic soils: effect of drying on the dispersion of the soils. Soil Sci. Plant Nutr. 18, 79–97. https://doi.org/10.1080/ 00380768 1972 10433277
- La Hora, D., 2004a. Lluvia afectó el sistema de alcantarillado en Cayambe [WWW Document]. La Hora Noticias de Ecuador, sus provincias y el mundo. URL. https://lahora.com.ec/noticia/1000285672/lluvia-afectc3b3-el-sistema-de-alcantarillado-en-cayambe, 12.16.21.
- La Hora, D., 2004b. Sequía afecta a sector agrario de Cayambe [WWW Document]. La Hora Noticias de Ecuador, sus provincias y el mundo. URL. https://lahora.com.ec/noticia/1000271870/sequc3ada-afecta-a-sector-agrario-de-cayambe, 12.16.21.
- Larrain Barros, H., 2016a. Cronistas de Raigambre Indígena e Hispánica. In: Biblioteca Cincuentenario IOA - Plutarco Cisneros Andrade, first ed. Instituto Otavaleño de Antropología, Otavalo, Ecuador.
- Larrain Barros, H., 2016b. Sierra Norte del Ecuador: Siglo XVI. Demografías y Asentamientos Indígenas (I). In: Biblioteca Cincuentenario IOA - Plutarco Cisneros Andrade, first ed. Instituto Otavaleño de Antropología, Otavalo, Ecuador.
- Le Pennec, J.-L., De Saulieu, G., Samaniego, P., Jaya, D., Gailler, L., 2013. A devastating Plinian eruption at Tungurahua Volcano reveals formative occupation at ~ 1100 cal BC in Central Ecuador. Radiocarbon 55. https://doi.org/10.1017/S0033822200048116.
- Linnaeus, C., 1758. Systema Naturae Per Regna Tria Naturae, Secundum Classes, Ordines, Genera, Species, Cum Characteribus, Differentiis, Synonymis, Locis, tenth ed. Laurentii Salvii, Holmiæ.
- Mena, V.P., Medina, G., Hofstede, R. (Eds.), 2001. Los Páramos del Ecuador: particularidades, problemas y perspectivas, first ed. Editorial Abya Yala/Proyecto Páramo, Ouito, Ecuador.
- Migeon, S., Garibaldi, C., Ratzov, G., Schmidt, S., Collot, J.-Y., Zaragosi, S., Texier, L., 2017. Earthquake-triggered deposits in the subduction trench of the north Ecuador/

- south Colombia margin and their implication for paleoseismology. Mar. Geol. 384, $47\text{--}62.\ https://doi.org/10.1016/j.margeo.2016.09.008.$
- Molestina, M. d, 1973. Toctiuco. Un sitio arqueológico en las faldas del Pichincha, 57. Boletín de la Academia Nacional de Historia, pp. 124–152.
- Molestina, M. del C., 2011. Interpretación Preliminar del Sitio Arqueológico Rumipamba. En: Rumipamba un sitio arqueológico en el corazón de Quito. Quito, Ecuador.
- Mook, W.G., Streurman, H.J., 1983. Physical and chemical aspects of radiocarbon dating. In: Proceedings of the First International Symposium 14 C and Archaeology, Groningen, pp. 31–55, 1981.
- Mothes, P., 1998. Actividad volcánica y pueblos precolombinos en el Ecuador. Editorial Abya Yala.
- Mothes, P.A., Hall, M.L., Janda, R.J., 1998. The enormous Chillos Valley lahar: an ash-flow-generated debris flow from Cotopaxi volcano, Ecuador. Bull. Volcanol. 59, 233–244. https://doi.org/10.1007/s004450050188.
- Municipal de Quito, Consejo, 1934. Actas de Cabildo de la Villa de San Francisco de Quito, año de 1539: Libro I, Actas de Cabildo de la Villa de San Francisco de Quito. Ouito. Ecuador.
- Newhall, C.G., Bronto, S., Alloway, B., Banks, N.G., Bahar, I., Marmol, M.A. del, Hadisantono, R.D., Holcomb, R.T., McGeehin, J., Miksic, J.N., Rubin, M., Sayudi, S. D., Sukhyar, R., Andreastuti, S., Tilling, R.I., Torley, R., Trimble, D., Wirakusumah, A.D., 2000. 10,000Years of explosive eruptions of Merapi Volcano, Central Java: archaeological and modern implications. J. Volcanol. Geoth. Res. 100, 9–50. https://doi.org/10.1016/S0377-0273(00)00132-3.
- Nocquet, J.-M., Villegas-Lanza, J.C., Chlieh, M., Mothes, P.A., Rolandone, F., Jarrin, P., Cisneros, D., Alvarado, A., Audin, L., Bondoux, F., Martin, X., Font, Y., Régnier, M., Vallée, M., Tran, T., Beauval, C., Maguiña Mendoza, J.M., Martinez, W., Tavera, H., Yepes, H., 2014. Motion of continental slivers and creeping subduction in the northern Andes. Nat. Geosci. 7, 287–291. https://doi.org/10.1038/ngeo2099.
- Nocquet, J.-M., Jarrin, P., Vallée, M., Mothes, P.A., Grandin, R., Rolandone, F., Delouis, B., Yepes, H., Font, Y., Fuentes, D., Régnier, M., Laurendeau, A., Cisneros, D., Hernandez, S., Sladen, A., Singaucho, J.-C., Mora, H., Gomez, J., Montes, L., Charvis, P., 2016. Supercycle at the Ecuadorian subduction zone revealed after the 2016 Pedernales earthquake. Nat. Geosci. https://doi.org/10.1038/ngeo2864.
- Nowak, R.M., 1999. Walker's mammals of the world. In: Walker's Mammals of the World, sixth ed. Johns Hopkins University Press, Baltimore, USA.
- Oberem, U., 1981. Los Caranquis de la sierra norte del Ecuador y su incorporación al Tahuantinsuyu. Contribución a la Etnohistória Ecuatoriana 72–101.
- Oberem, U., Wurster, W.W., 1989. Excavaciones en Cochasquí, Ecuador, 1964-1965. Verlag Philipp von Zabern, Mainz, Germany.
- Ontaneda, S., 2002. El cacicazgo Panzaleo como parte del área circumquiteña. Banco Central del Ecuador, Quito.
- Ontaneda, S., 2010. Historia de los Pueblos precolombinos de la Sierra Norte del Fruador. Quito: Banco Central del Ecuador.
- Orton, C., Hughes, M., 2013. Pottery in Archaeology, second ed. Cambridge University Press, New York, USA.
- Peacock, D.P.S., 1977. Pottery and early commerce: characterization and trade in roman and later ceramics. Stud. Archaeol. Sci. Academic Press.
- Peltre, P., 1989. Quebradas y riesgos naturales en Quito, período 1900-1988. In: Riesgos Naturales en Quito, Lahares, aluviones y derrumbes del Pichincha y del Cotopaxi. Corporación Editora Nacional, Quito, Ecuador, p. 25.
- Pourrut, P., 1998. El Niño 1982-1983 a la luz de las enseñanzas de los eventos del pasado-impactos en el Ecuador, 27. Bulletin de l'institut Francais d'Etudes Andines. https://www.redalyc.org/pdf/126/12627315.pdf.
- Ramon, P., Vallejo Vargas, S., Mothes, P.A., Andrade, S.D., Vasconez, F.J., Yepes, H., Hidalgo, S., Santamaría, S., 2021. Instituto Geoffsico – Escuela Politécnica Nacional, the Ecuadorian seismology and volcanology service. Volcanica, Volcano Observatories in Latin America 4, 93–112. https://doi.org/10.30909/vol.04. S1.93112.
- Reimer, P.J., Austin, W.E.N., Bard, E., Bayliss, A., Blackwell, P.G., Bronk Ramsey, C., Butzin, M., Cheng, H., Edwards, R.L., Friedrich, M., Grootes, P.M., Guilderson, T.P., Hajdas, I., Heaton, T.J., Hogg, A.G., Hughen, K.A., Kromer, B., Manning, S.W., Muscheler, R., Palmer, J.G., Pearson, C., Plicht, J. van der, Reimer, R.W., Richards, D.A., Scott, E.M., Southon, J.R., Turney, C.S.M., Wacker, L., Adolphi, F., Büntgen, U., Capano, M., Fahrni, S.M., Fogtmann-Schulz, A., Friedrich, R., Köhler, P., Kudsk, S., Miyake, F., Olsen, J., Reinig, F., Sakamoto, M., Sookdeo, A., Talamo, S., 2020. The IntCal20 northern Hemisphere radiocarbon age calibration curve (0–55 cal kBP). Radiocarbon 62, 725–757. https://doi.org/10.1017/RDC.2020.41.
- Retallack, G.J., 2001. Soils of the Past: an Introduction to Paleopedology, second ed. Blackwell Science, Oxford; Malden, MA.
- Reyes, P., Procel, S., Sevilla, J., Cabero, A., Orozco, A., Córdova, J., Lima, F., Vasconez, F., 2021. Exceptionally uncommon overburden collapse behind a natural lava dam: abandonment of the San-Rafael Waterfall in northeastern Ecuador. J. S. Am. Earth Sci. 110, 103353 https://doi.org/10.1016/j.jsames.2021.103353.
- Riede, F., 2008. The laacher see-eruption (12,920 BP) and material culture change at the end of the Allerød in northern Europe. J. Archaeol. Sci. 35, 591–599. https://doi. org/10.1016/j.jas.2007.05.007.
- Riede, F., 2016. Volcanic activity and human society. Quat. Int. 394, 1–5. https://doi.org/10.1016/j.quaint.2015.08.090.
- Riede, F., Barnes, G.L., Elson, M.D., Oetelaar, G.A., Holmberg, K.G., Sheets, P., 2020. Prospects and pitfalls in integrating volcanology and archaeology: a review. J. Volcanol. Geoth. Res. 401, 106977 https://doi.org/10.1016/j. jvolgeores.2020.106977.
- Robin, C., Eissen, J.-P., Samaniego, P., Martin, H., Hall, M., Cotten, J., 2009. Evolution of the late Pleistocene Mojanda–Fuya Fuya volcanic complex (Ecuador), by progressive

- adakitic involvement in mantle magma sources. Bull. Volcanol. 71, 233–258. https://doi.org/10.1007/s00445-008-0219-9.
- Rosi, M., Levi, S.T., Pistolesi, M., Bertagnini, A., Brunelli, D., Cannavò, V., Di Renzoni, A., Ferranti, F., Renzulli, A., Yoon, D., 2019. Geoarchaeological evidence of middle-age tsunamis at Stromboli and consequences for the tsunami hazard in the southern Tyrrhenian sea. Sci. Rep. 9, 677. https://doi.org/10.1038/s41598-018-37050-3.
- Samaniego, P., 2004. Escuela Politécnica Nacional (Quito, Ecuador), Institut de recherche pour le développement (France). In: Los peligros volcánicos asociados con el Cayambe, Los peligros volcánicos en el Ecuador. Corporación Editora Nacional, Ouito, Ecuador.
- Samaniego, P., Monzier, M., Robin, C., Hall, M.L., 1998. Late Holocene eruptive activity at Nevado Cayambe volcano, Ecuador. Bull. Volcanol. 59, 451–459. https://doi.org/ 10.1007/s004450050203.
- Samaniego, P., Monzier, M., Robin, C., Eissen, J.-P., Hall, M.L., Mothes, P.A., Yepes, H., 2002. Mapa de los Peligros Potenciales del Volcán Cayambe.
- Samaniego, P., Martin, H., Monzier, M., Robin, C., Fornari, M., Eissen, J.-P., Cotten, J., 2005. Temporal evolution of magmatism in the northern volcanic zone of the Andes: the geology and petrology of Cayambe volcanic complex (Ecuador). J. Petrol. 46, 2225–2252. https://doi.org/10.1093/petrology/egi053.
- Sánchez, M.V., Genise, J.F., Bellosi, E.S., Román-Carrión, J.L., Cantil, L.F., 2013. Dung beetle brood balls from Pleistocene highland palaeosols of Andean Ecuador: a reassessment of Sauer's Coprinisphaera and their palaeoenvironments. Palaeogeogr. Palaeoclimatol. Palaeoecol. 386, 257–274. https://doi.org/10.1016/j. palaeo.2013.05.028.
- Sandoval, C., 2020. Estudio internacional sugiere reubicar obras por la erosión [WWW Document]. El Comercio. URL. https://www.elcomercio.com/actualidad/negocios/estudio-reubicacion-obras-erosion-coca.html, 11.9.21.
- Schobinger, J., 1988. Prehistoria de Sudamérica: culturas precerámicas. Alianza Editorial, Madrid.
- Schuster, R.L., NietoThomas, A.S., O'Rourke, T.D., Crespo, E., Plaza-Nieto, G., 1996. Mass wasting triggered by the 5 March 1987 Ecuador earthquakes. Eng. Geol. 42, 1–23. https://doi.org/10.1016/0013-7952(95)00024-0.
- Scott, K.M., Vallance, J.W., Pringle, P.T., 1995. Sedimentology, Behavior, and Hazards of Debris Flows at Mount Rainier. US Geological Survey, Washington.
- Shoji, S., Dahlgren, R., Nanzyo, M., 1993. Genesis of volcanic ash soils. In: Developments in Soil Science. Elsevier, pp. 37–71.
- Siebe, C., Abrams, M., Macías, J.L., Obenholzner, J., 1996. Repeated volcanic disasters in Prehispanic time at Popocatepetl, central Mexico: past key to the future? Geology 24, 4. https://doi.org/10.1130/0091-7613(1996)024<0399:RVDIPT>2.3.CO;2.
- Sigurdsson, H., Cashdollar, S., Sparks, S.R.J., 1982. The eruption of Vesuvius in A. D. 79: reconstruction from historical and volcanological evidence. Am. J. Archaeol. 86, 39. https://doi.org/10.2307/504292.
- Skibo, J.M., 1992. Pottery Function: a Use-Alteration Perspective. Springer Science & Business Media.
- Smith, V.C., Staff, R.A., Blockley, S.P., Ramsey, C.B., Nakagawa, T., Mark, D.F., Takemura, K., Danhara, T., 2013. Identification and correlation of visible tephras in the Lake Suigetsu SG06 sedimentary archive, Japan: chronostratigraphic markers for synchronising of east Asian/west Pacific palaeoclimatic records across the last 150 ka. Quat. Sci. Rev. 67, 121–137. https://doi.org/10.1016/j.quascirev.2013.01.026.
- Stuiver, M., Reimer, P.J., 1986. A computer program for radiocarbon age calibration. Radiocarbon 28, 1022–1030. https://doi.org/10.1017/S0033822200060276.
- Stuiver, M., Reimer, P.J., Reimer, R.W., 2021. CALIB 8.2 [WWW program]. USA.

- Stübel, A., Reiss, 1987. Las Montañas Volcánicas del Ecuador Retratadas y descritas Geológica Topográficamente, UNESCO. In: Archivo Histórico del Banco Central del Ecuador.
- Talma, A.S., Vogel, J.C., 1993. A simplified approach to calibrating ¹⁴ C dates. Radiocarbon 35, 317–322. https://doi.org/10.1017/S0033822200065000.
- Tibaldi, A., Ferrari, L., Pasquarè, G., 1995. Landslides triggered by earthquakes and their relations with faults and mountain slope geometry: an example from Ecuador. Geomorphology 11, 215–226. https://doi.org/10.1016/0169-555X(94)00060-5.
- Tibaldi, A., Rovida, A., Corazzato, C., 2007. Late Quaternary kinematics, slip-rate and segmentation of a major Cordillera-parallel transcurrent fault: the Cayambe-Afiladores-Sibundoy system, NW South America. J. Struct. Geol. 29, 664–680. https://doi.org/10.1016/j.jsg.2006.11.008.
- Tirira, D., 2007. Guía de campo de los mamíferos del Ecuador. Ediciones Murciélago Blanco 6, 576. Publicación especial sobre los mamíferos del Ecuador.
- Ugalde, M.F., 2017. Volcanes, cenizas y ocupaciones antiguas en perspectiva geoarqueológica en América Latina, Estudios de Antropología y Arqueología. Centro de Publicaciones Pontificia Universidad Católica del Ecuador, Quito, Ecuador.
- Vásconez, R., Hall, M., Mothes, P.A., 2009. Devastadores flujos de lodo disparados en el volcán Carihuairazo por el terremoto del 20 de Junio de 1698. Revista Politécnica 20
- Vasconez, F.J., Vásconez, R., Mothes, P.A., 2022. Flujos de lodo del volcán Carihuairazo provocados por el terremoto de Ambato, Ecuador, en 1698 y su reconstrucción numérica con perspectivas a futuro. Rev. Geofisc. 1, 20. https://doi.org/10.35424/ ref.v0i69.937.
- Villalba, M., 1988. Cotocollao: una aldea formativa del valle de Quito. Museos del Banco central del Ecuador.
- Villalba, F., Domínguez, V., 2009. Estudio Funcional de Camellones, un Sistema Agrícola Precolombino en la Sierra Norte del Ecuador, 9. Período de Integración).
- Vizuete, N., 2020. Geocronología, parámetros eruptivos de fuente y dinámica del evento "San Marcos" del volcán Cayambe. Escuela Politécnica Naciona, Quito, Ecuador.
- Vogel, A., Diplas, S., Durant, A.J., Azar, A.S., Sunding, M.F., Rose, W.I., Sytchkova, A., Bonadonna, C., Krüger, K., Stohl, A., 2017. Reference data set of volcanic ash physicochemical and optical properties. J. Geophys. Res. Atmos. 122, 9485–9514. https://doi.org/10.1002/2016JD026328.
- Winckell, A., Zebrowski, C., 1992. La cangahua en Equateur: le contexte paléogéographique de sa formation. Terra 10, 107–112.
- Witt, C., Bourgois, J., Michaud, F., Ordoñez, M., Jiménez, N., Sosson, M., 2006. Development of the Gulf of Guayaquil (Ecuador) during the quaternary as an effect of the north andean block tectonic escape: development of the Gulf of Guayaquil. Tectonics 25. https://doi.org/10.1029/2004TC001723 n/a -n/a.
- Wolf, T., 1873. Crónica de los fenómenos volcánicos y terremotos en el Ecuador con algunas noticias sobre otros países de la América Central y Meridional desde 1535 hasta 1797. Escuela Politécnica Nacional, Quito, Ecuador
- Zehetner, F., Miller, W.P., West, L.T., 2003. Pedogenesis of volcanic ash soils in andean Ecuador. Soil Sci. Soc. Am. J. 67, 1797–1809. https://doi.org/10.2136/ sssai2003.1797.
- Zeidler, J.A., 2016. Modeling cultural responses to volcanic disaster in the ancient Jama–Coaque tradition, coastal Ecuador: a case study in cultural collapse and social resilience. Ouat. Int. 394, 79–97. https://doi.org/10.1016/j.quaint.2015.09.011.
- Zevallos, O., Fernández, M.A., Plaza Nieto, G., Klinkicht Sojos, S., 1996. Sin plazo para la esperanza: reporte sobre el Desastre de la Josefina-Ecuador, 1993. In: Sin plazo para la esperanza: Reporte sobre el Desastre de la Josefina-Ecuador, 1993. Escuela Politécnica Nacional, Ecuador, p. 348.